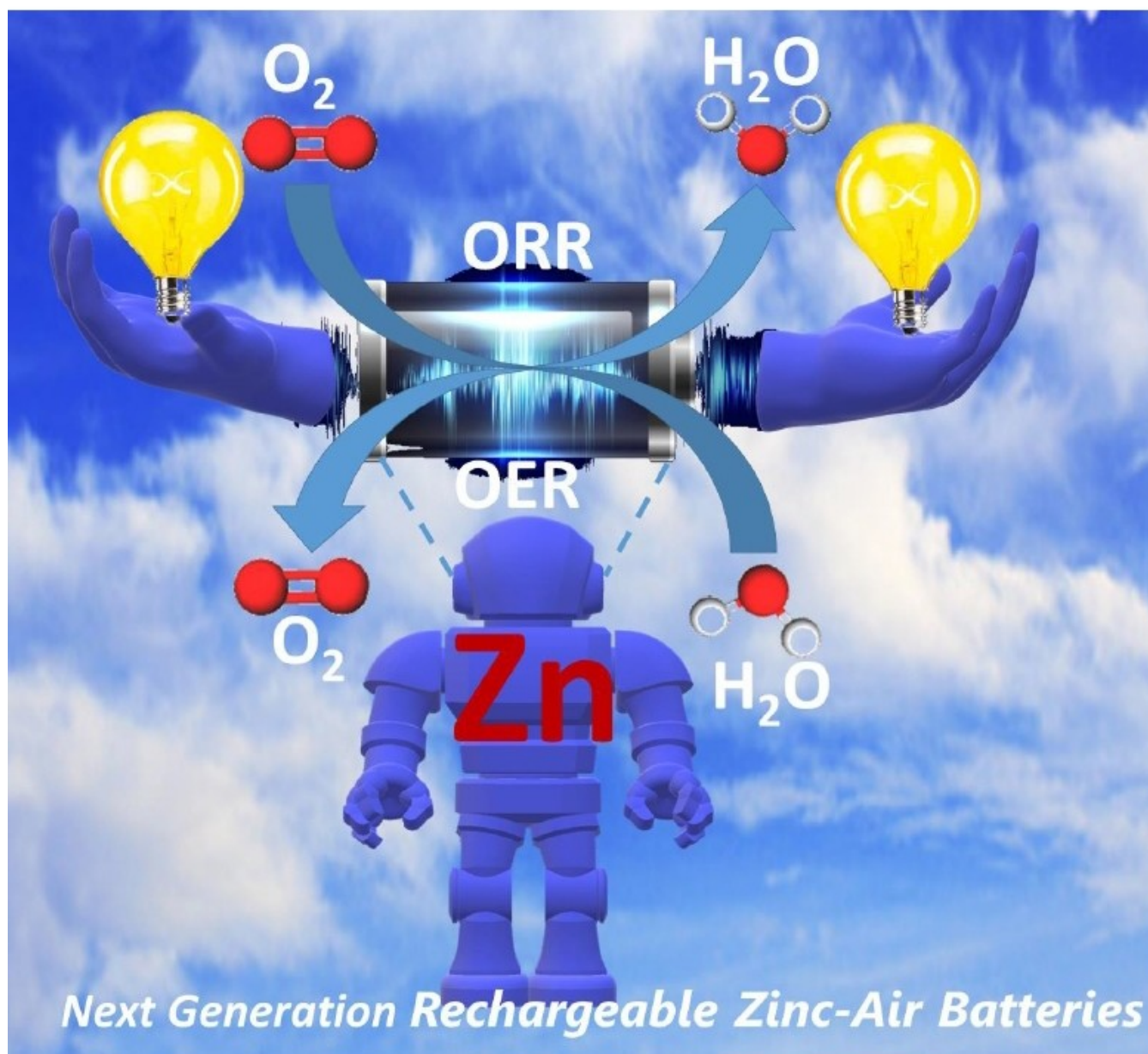VIP *Very Important Paper*

Efforts at Enhancing Bifunctional Electrocatalysis and Related Events for Rechargeable Zinc-Air Batteries

Adewale K. Ipadeola,[a] Aderemi B. Haruna,[a] Lesego Gaolatlhe,[a] Augustus K. Lebechi,[a] Jiashen Meng,[b] Quanquan Pang,*[b] Kamel Eid,*[c] Aboubakr M. Abdullah,[d] and Kenneth I. Ozoemena*[a]

ChemElectroChem

Review
doi.org/10.1002/celc.202100574

Chemistry Europe
European Chemical
Societies Publishing

Rechargeable zinc-air batteries (RZABs) are one of the most promising next-generation energy-storage technologies for stationary applications (home and industry), wearable and portable electronics, and transportation (including electric vehicles) due to their high energy density, environmental friendliness, safety, and low cost. However, RZABs still face serious challenges (such as sluggish oxygen reactions, poor durability, inferior reversibility of the zinc anode, and low cell energy efficiency) that conspire against their widespread commercialization. The reactions that occur at the three key components of the RZAB (air cathode, zinc anode, and electrolyte) co-operatively conspire against its performance. Thus, this review focuses on the bifunctional electrocatalytic events at the cathode (i.e., oxygen reduction reaction (ORR) and oxygen evolution reaction (OER)). That is in addition to the recent developments aimed at mitigating the performance-limiting events at the anode and the electrolytes. This review directs the attention of researchers and users to the critical areas for the development of the next-generation RZABs.

1. Introduction

The increasing energy consumption in this modern age is a serious concern for developing sustainable energy systems. Metal-air batteries, particularly rechargeable zinc-air batteries (RZABs) have emerged as one of the next-generation hybrid energy conversion and storage systems that utilize a configuration combining fuel cells and batteries with high energy integrity to meet the huge demands globally.[1] RZAB was initially discovered in the 19th century and has been successfully commercialized for medical and telecommunication applications like portable hearing aids and wireless messaging devices.[2,3] However, it is poorly explored for the large-scale energy systems as its development remains in infancy. Hence, there is still much development and exploration needed to bring the RZAB to the limelight of energy systems. One of such areas of development is the bifunctional electrocatalysts that can drive ORR and OER in alkaline media, considering that alkaline environments offer unique advantages.[4] For example, for fast ORR kinetics, reduced risks of corrosions, and the opportunity to utilize low-cost non-precious metal electrocatalysts. The RZABs have intriguing characteristics of relatively low cost, improved safety with minimal environmental impacts than other metal-air batteries, additionally, the RZABs have high theoretical and specific energy densities (500 Wh kg$^{-1}_{cell}$ and 1400 Wh L$^{-1}_{cell}$) compared to commercial Li-ion batteries (LIB, 350 Wh Kg$^{-1}_{cell}$ and 810 Wh L$^{-1}_{cell}$),[5,6] making them viable energy storage systems in various applications such as wearable and portable devices and electric vehicles (EVs).[7]

In the last decade, the development of bifunctional electrocatalysts has led to increased research activities on RZABs, resulting in nearly 645 articles according to Web of Science (Figure 1). Thus, it is critical to provide an update on the recent progress in the area of rechargeable zinc-air batteries. Although there are a number of reviews about RZABs published recently, most of them focused purely on the bifunctional catalysts for the oxygen reduction (ORR) and oxygen evolution reactions (OER) in RZABs, without highlighting the rational design of RZABs as a whole or modulating their performance and durability from a systematic point of view.[8–12]

In pursuit of this aim, this review discusses the fabrication methods of highly efficient RZABs. The discussion roots from the fundamental mechanism of Zn anode and cathode reactions to introduce the current challenges (i.e., dendrite growth, shape change, passivation, and H$_2$ evolution) (Scheme 1). The syntheses of bifunctional air electrocatalysts toward ORR and OER are subsequently discussed, followed by the electrolytes design (i.e., aqueous, non-aqueous, solid-state, and hybrid electrolytes). Finally, we offer our perspectives on the future development of the RZABs (Scheme 1).

[a] Dr. A. K. Ipadeola, Dr. A. B. Haruna, L. Gaolatlhe,[+] A. K. Lebechi,[+]
     Prof. K. I. Ozoemena
     Molecular Sciences Institute, School of Chemistry
     University of the Witwatersrand
     Private Bag 3, PO Wits, Johannesburg 2050, South Africa
     E-mail: kenneth.ozoemena@wits.ac.za
[b] Dr. J. Meng, Prof. Q. Pang
     School of Materials Science and Engineering
     Peking University
     Beijing, 100871, China
     E-mail: qqpang@pku.edu.cn
[c] Dr. K. Eid
     Gas Processing Centre, College of Engineering
     Qatar University
     Doha 2713, Qatar
     E-mail: kamelame@outlook.com
[d] Prof. A. M. Abdullah
     Centre for Advanced Materials, College of Engineering
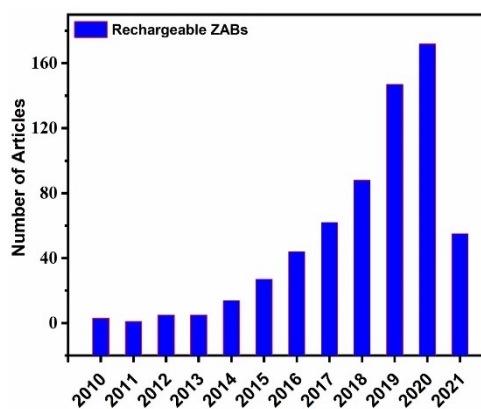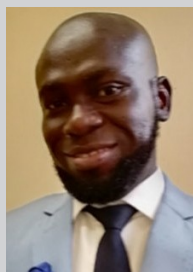   Qatar University
     Doha 2713, Qatar

Figure 1. The articles related to rechargeable ZABs that were published between 2010 and 15th April 2021, obtained from Web of Science data using these keywords "rechargeable zinc-air batteries".

ChemElectroChem

Review
doi.org/10.1002/celc.202100574

Chemistry Europe
European Chemical
Societies Publishing

Dr. Adewale Kabir Ipadeola obtained his BSc (Hons) and MSc degrees in Chemistry (cum laude) from the Lagos State University and University of Lagos, respectively. In 2018 he joined the group of Prof KI Ozoemena at the School of Chemistry, University of the Witwatersrand (Wits) for his PhD studies. He earned his Ph.D degree (Chemistry) in 2020 and is currently a Postdoctoral Research Fellow with research interests in electrocatalysis, fuel cells, and rechargeable metal-air batteries. Dr Ipadeola has over seven years of experiences in teaching and research, and has published some peer-reviewed articles.

Dr. Aderemi Bashiru Haruna is currently a Postdoctoral Research Fellow in the group of Prof KI Ozoemena at the University of the Witwatersrand (Wits), Johannesburg, South Africa. He obtained his PhD at Wits in 2020, which focussed on manganese-based spinel cathode materials for lithium-ion batteries. His current research interests lie in the fields of energy storage, including lithium-ion, sodium-ion, lithium-sulphur, and zinc-air batteries. He is also interested in exploring green chemistry synthesis methods (especially microwave-assisted synthesis) aimed at tuning the physico-chemistry and interfacial electrochemistry of the electrode materials.
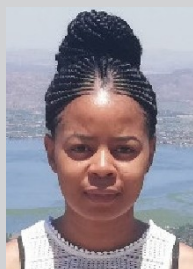
Lesego Gaolatlhe obtained her BSc (Hons) Chemistry from the North-West University, Mafikeng (South Africa). In 2019 she joined the group of Prof KI Ozoemena at the University of the Witwatersrand (Wits) and obtained her MSc in Chemistry (cum laude) in 2020. She is currently a PhD candidate at Wits with research interests in sensors, electrocatalysis, and rechargeable zinc-air batteries.

Augustus Kelechi Lebechi obtained his BSc (Hons) and MSc degrees in Chemistry (cum laude) from Rhodes University, Grahamstown (South Africa) in 2017 and 2020, respectively. He is currently pursuing his PhD studies at the University of the Witwatersrand under the supervision of Prof KI Ozoemena. His current research interests are in electrocatalysis and rechargeable metal-air batteries.
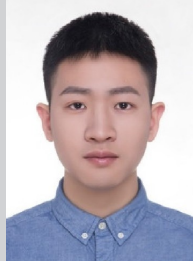
Jiashen Meng is now a Postdoctoral Research Fellow at Peking University starting 2020 under the supervision of Prof. Quanquan Pang and Ruqiang Zou. He received his B.S. and Ph.D. degrees in materials science and engineering under the supervision of Prof. Liqiang Mai from Wuhan University of Technology in 2015 and 2020, respectively. In 2018–2019, He was a visiting Ph.D. student at MIT. His current research focuses on developing new nanomaterials and chemical solutions for extreme batteries.

Dr. Quanquan Pang is currently an Assistant Professor in the School of Materials Science and Engineering at Peking University. He received his Ph. D. in Chemistry under the supervision of Prof. Linda F. Nazar from University of Waterloo in 2017, working on the many aspects of lithium-sulfur battery. He then completed his postdoctoral research at Massachusetts Institute of Technology before joining Peking University in 2020. His current research interests include the materials chemistry and electrochemistry in a variety of energy storage systems, including zinc-air batteries, metal-sulfur batteries, multi-valent batteries, and solid-state batteries.

Dr. Kamel Eid received his Bachelor's, Master's, and Ph.D. degrees from Al-Azhar University in Egypt (2005), Helwan University in Egypt (2011), and the Chinese academy of sciences in China (2016), respectively. He is currently a Research Associate at the Gas Processing Center, College of Engineering, Qatar University in Qatar. He serves as a visiting Assistant Professor at several universities and has published over 68 SCI-cited papers in prestigious international journals and filled 11 US patents in the field of electrocatalysis, electrochemical energy conversion technologies, fuel cells, and water treatment.

Dr. Aboubakr has awarded his BSc and MSc from Cairo University, Egypt in 1993 and 1997, respectively, and PhD in Materials Science and Engineering from Pennsylvania State University, USA in 2003. Subsequently, he worked as a Postdoc in Kuwait University, Kuwait; Tokyo Institute of Technology, Japan; and University of Calgary, AB, Canada. He is currently a Hydro/Qatalum Chair Professor Center for Advanced Materials Qatar University. He has published over 130 SCI-cited papers with (h-index of 24) and filled 10 US patents.

Kenneth Ikechukwu Ozoemena is Research Professor and South African Research Chair Initiative (SARChI) Chair (Tier 1) in Materials Electrochemistry and Energy Technologies (MEET) at the University of the Witwatersrand, South Africa. His research is focussed on advanced batteries, fuel cells and electrochemical sensors. He holds a PhD (Chemistry) degree from Rhodes University (2003). He is a member of the national Academy of Science of South Africa (ASSAf), Fellow of the African Academy of Science (FAAS), and Fellow of the Royal Society of Chemistry (FRSC), and a Fellow of the Association of Commonwealth Universities at Coventry University, UK (2021). He serves on the Editorial Board of Electrochemistry Communications (Elsevier), Current Opinion in Electrochemistry (Elsevier), and Scientific Reports (Nature Publishing), Catalysis (MPDI Publishing) and Chief Editor, International Journal of Electrochemistry (Wiley/Hindawi Publishing).
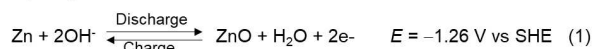
ChemElectroChem

Review
doi.org/10.1002/celc.202100574

Chemistry Europe
European Chemical
Societies Publishing

Scheme 1. The main sections discussed in this review.

Figure 2. Schematic shows the proposed working principle of rechargeable zinc-air battery (RZAB) using a nanoporous bifunctional electrocatalyst that drives the ORR/OER of the battery.
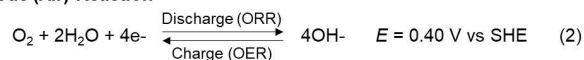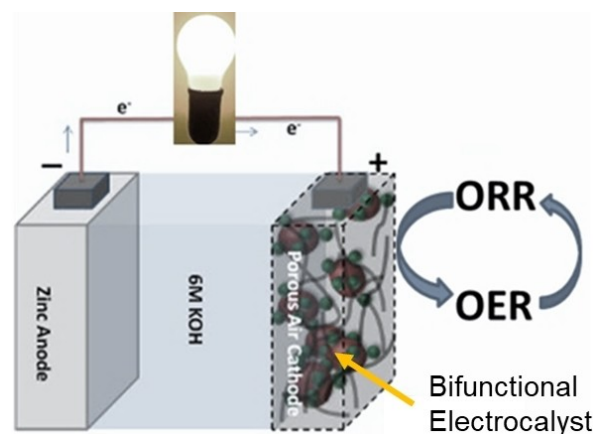
1.1. Configuration and Working Principle of Rechargeable Zinc-Air Batteries

The rechargeable ZABs consist of (i) the zinc (Zn) anode, which serves as the fuel; (ii) the electrolyte that allows ion-migration during charging-discharging processes; (iii) the separator that restrains physical inter-crossing of the anode and cathode and selectively allows migration of the charge-carrier ions; and (iv) the air electrode which serves as the cathode where oxygen (O_2) electrochemistry occurs, i.e., ORR and OER, controlling the reaction kinetics for discharging and charging, respectively.[13,14] The anode and cathode reactions are summarized in Equations (1)–(3):

Anode (Zinc) Reaction

$$Zn + 2OH^- \underset{Charge}{\overset{Discharge}{\rightleftarrows}} ZnO + H_2O + 2e^- \qquad E = -1.26 \text{ V vs SHE} \quad (1)$$

Cathode (Air) Reaction

$$O_2 + 2H_2O + 4e^- \underset{Charge (OER)}{\overset{Discharge (ORR)}{\rightleftarrows}} 4OH^- \qquad E = 0.40 \text{ V vs SHE} \quad (2)$$

Overall Reaction

$$2Zn + O_2 \underset{Charge}{\overset{Discharge}{\rightleftarrows}} 2ZnO \qquad E_{cell} = 1.66 \text{ V vs SHE} \quad (3)$$

Following the ZAB's configuration shown in Figure 2, upon discharge, the Zn anode gets oxidized to form soluble Zn hydroxides ($Zn(OH)_4^{2-}$, also known as zincate ions) that spontaneously decomposes to form insoluble Zn oxide (ZnO); in the cathode, O_2 from the atmosphere penetrates through the porous air electrode to undergo ORR. Upon charge, Zn is plated at the anode, and OER occurs at the cathode. The sluggishness of ORR and OER kinetics necessitates the development and use of bifunctional air electrocatalysts, which need to be highly active and durable for the O_2 electrochemistry. Efficient and effective bifunctional electrocatalysts in the RZABs improve its performance, stability, and recyclability.

1.2. Challenges in Rechargeable Zinc-Air Batteries (RZABs)

Although the RZABs have numerous prospects as an energy storage system, their practical development has been conspired with many setbacks on each of the major components. Efforts have been largely devoted to identifying the drawbacks on the major components: Zn anode, air electrode, and electrolytes, as highlighted below:

(i) The Zn anode of the RZABs is prone to dendrites growth, i.e., deposition of crystalline protruded Zn metals during charging process leading to short-circuiting of the battery;[15] formation of irreversible ZnO during discharging process;[16] zincate ion cross-over and generation of hydrogen gas (H_2) from water (H_2O) via hydrogen evolution reaction (HER) leading to Zn corrosion and rapid passivation. Recent efforts toward enhancing the anode's efficiency involve mitigating the dendrites growth and suppressing the hydrogen generation by electroplating or alloying the Zn metal with other materials such as a carbon nano-disc layer and additives.[17,18] The ZnO formation can be inhibited by reducing the depth of discharge or employing zincate ion scavengers (like $Ca(OH)_2$, PdO, silicate etc.) to remove excess zincate ions and to prevent their cross-over.[19,20]

(ii) The air electrode serves as the cathode where ORR and OER reactions occur with poor kinetics evidenced by high overpotentials, low coulombic efficiency, and poor durability,[5] hence requiring bifunctional electrocatalysts that are both active and stable to O_2 electrochemistry and have lower overpotentials. Various efforts have been dedicated to providing highly active and durable bifunctional electrocatalysts for the ORR and OER to prevent the air electrode from degradation.

(iii) The electrolytes and membranes design: The electrolytes employed in the RZABs could be aqueous, non-aqueous, and solid-state electrolytes. Low coulombic efficiency is partially ascribed to the Zn anode corrosion, especially in alkaline aqueous electrolytes,[21] and water splitting at high

ChemElectroChem

Review
doi.org/10.1002/celc.202100574

Chemistry
Europe
European Chemical
Societies Publishing

overpotential during charging.[22] Thus, rational design of the electrolytes is necessary for high coulombic efficiency. Amongst the efforts were using electrolyte additives to prevent the electrolysis of water and carbonation at the overpotential range of the RZAB.[23]

Giving the highlighted significant challenges on the components of the RZABs, progresses on solutions proposed to resolve each and all the challenges are discussed in subsequent sections. It is imperative to note that recent reviews on the RZABs have provided the summary of major components of the RZABs with mechanism, challenges and possible solutions with so much attention on the Zn anode and bifunctional electrocatalysts at the air electrode, but little or no attention on the electrolyte's contributions, as an alkaline electrolyte is always reported.[5,6] The need to comprehensively discuss the overall challenges at the three major components of the RZABs necessitated this review.

2. Zinc Anode

The RZABs are mainly considered for large-scale grid systems because the Zn anode is cheap, safe, easy to recycle, and electrochemically reversible.[25] The Zn metal also has a high capacity of 820 mAh g^{-1} and volumetric capacity of 5854 mAh cm^{-3},[24] low redox potential of -0.762 V (vs. standard hydrogen electrode, SHE), and it shows a large HER overpotential in aqueous electrolytes.[26]

2.1 Zinc Anode Reaction Mechanism

Zn anode reactions in RZABs can occur either in the alkaline or mildly acidic electrolytes.

Discharge/Charge Processes in Alkaline Electrolyte:[26,27]

*Electro-oxidation:* During the discharge process, the Zn metal losses two electrons (e$^-$) to form Zn^{2+} ions.

$$Zn \rightarrow Zn^{2+} + 2e^- \tag{4}$$

Complexation: The Zn^{2+} ions react with the OH$^-$ in the alkaline electrolyte to form Zn(OH)$_4^{2-}$ ions.

$$Zn^{2+}_{(aq)} + 4OH^-_{(aq)} \rightarrow Zn(OH)_4^{2-}_{(aq)} \tag{5}$$
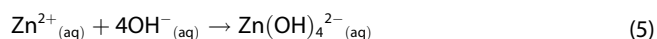
Dehydration/Precipitation: As the above equation (5) proceeds, the Zn(OH)$_4^{2-}_{(aq)}$ concentration in electrolyte increases; hence when the Zn(OH)$_4^{2-}$ ions reach saturation, they decompose to insoluble ZnO$_{(s)}$ on the surface of the negative electrode, as given below.

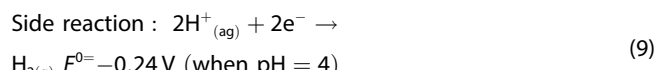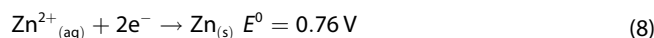$$Zn(OH)_4^{2-}_{(aq)} \rightarrow ZnO_{(s)} + H_2O_{(l)} + 2OH^-_{(aq)} \tag{6}$$
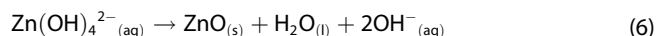
The overall reaction of Zn anode during the discharging/charging process in the alkaline electrolyte is given in Equation (1). However, it is pertinent to note that HER side reaction occurs at the zinc anode as given in Equation (7):

$$Zn + 2H_2O \rightarrow H_{2(g)} + Zn(OH)_2 \rightarrow$$
$$E^0 = -0.83 \text{ V vs SHE (at pH 14)} \tag{7}$$
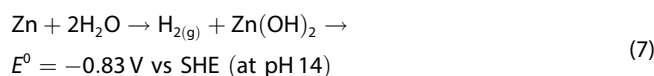
Equation 1 shows that the standard reduction potential of ZnO/Zn (-1.26 V) is lower than that of the HER (Equation (7), -0.83 V), which means that HER is a thermodynamically favoured reaction and almost always accompany the Zn plating reactions; and even when a Zn anode is at rest, corrosion still occurs (i.e., self-discharge) over time. This is the reason why it is difficult to charge a Zn anode with 100% Coulombic efficiency.

Discharge/Charge Processes in Mildly Acidic Electrolyte:

The Zn oxidizes to Zn^{2+} ions with e$^-$ losses. The reactions during the charging process are the reverse of the discharging process as given in Equation (8). In addition, the H$^+$ ions in the mildly acidic electrolyte also gets reduced to H$_2$ (Equation (9)).[26]

$$Zn^{2+}_{(aq)} + 2e^- \rightarrow Zn_{(s)} \ E^0 = 0.76 \text{ V} \tag{8}$$

$$\text{Side reaction}: \ 2H^+_{(ag)} + 2e^- \rightarrow$$
$$H_{2(g)} \ E^{0=} -0.24 \text{ V (when pH} = 4) \tag{9}$$

Zn anode reactions in mildly acidic electrolytes (pH ~4) are much easier than those in the alkaline electrolytes.[26] Unfortunately, however, developing RZAB in the mild electrolyte has been fraught with many challenges because of the lack of efficient bifunctional electrocatalysts under mild conditions. In the alkaline media, the catalytic performance of bifunctional electrocatalysts increased substantially results in fast oxygen reactions kinetics and reduced risks of corrosion.[4] Therefore, it is more important to develop alkaline-based RZABs than mild-acid-based RZABs.

2.2. Current Progress on Zinc Anodes in Rechargeable Zinc-Air Batteries

The practical application of RZABs is hindered by the poor rechargeability of Zn anodes. This drawback can be attributed to the challenges that accompany the use of Zn i.e., dendrite growth, shape change, passivation, and H$_2$ evolution, as illustrated in Figure 3.[27] Therefore, it is imperative to review the current progress made to ameliorate these challenges, as shown in Figure 4, elucidated and summarized in Table 1.
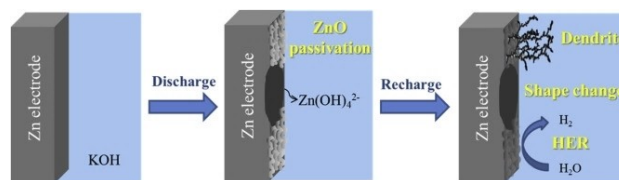

Figure 3. Schematic of the challenges of rechargeable Zn electrodes. Reproduced with permission from Ref. [27]: Copyright (2019) Elsevier.

ChemElectroChem

Review
doi.org/10.1002/celc.202100574

**Chemistry
Europe**
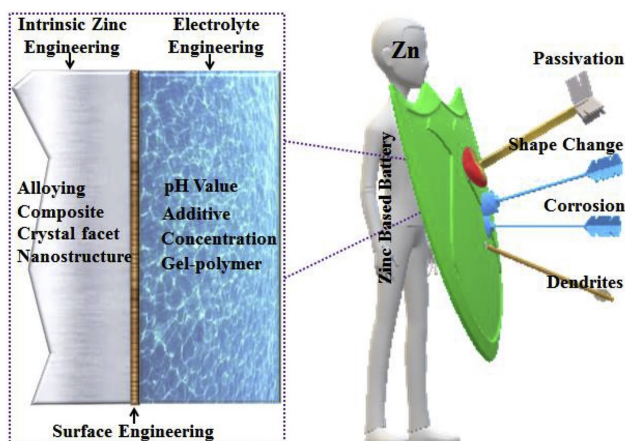European Chemical
Societies Publishing

Figure 4. Schematic strategies adopted to mitigate the challenges of Zn anode in the RZABs. "Reprinted with permission from Ref. [25]. Copyright (2020) Elsevier".

Amongst the strategies adopted to mitigate these challenges was the use of polymers and electrolytes additives. For instance, Wang and co-workers[28] reported that electrolyte additives like benzotriazole (BTA), tetrabutylammonium bromide (TBAB), and a combination of the two impeded dendrites growth, passivation, H$_2$ generation, and corrosion. The study revealed optimum RZAB electrochemical performance for the electrolyte with 100 mg L^{-1} BTA and 50 mg L^{-1} TBAB, showing an increased specific capacity of 475.6 mAh g^{-1} compared to that without additives (327.3 mAh g^{-1}) and capacity retention of 83.2% after the 50th cycles. Huang et al.[29] designed a novel multiphase alkaline ZAB electrolyte to prevent the growth of dendrites. In this study, the Zn anode and air electrode were positioned or enclosed in the heterogeneous and homogeneous phases of the alkaline electrolytes, respectively. The designed ZAB has energy densities of 196.2 W kg^{-1} and 309.1 Wh L^{-1} with outstanding capacity retention of 100% after 10,000 cycles at 50 mA cm^{-2}. Mainar et al.[30] used a single strategy of modified alkaline electrolyte to mitigate the high solubility of zinc; however, it does improve the cycle life of RZAB. Therefore, the group used a combination of anode coating with ionomer and electrolyte additives to mitigate the Zn anode exposure, zincate ion solubility, shape change, dendrite growth, and HER. The combined strategies showed that the coated Zn anode in the modified electrolyte has a reduced corrosion rate (1.3 mg$_{Zn}$ cm^{-1} s^{-1}) compared to the blank (10.4 mg$_{Zn}$ cm^{-1} s^{-1}) and high specific energy of 25 Wh kg^{-1}$_{Zn}$. In addition, the coated Zn anode has increased cycle life and roundtrip energy efficiency greater than 55% after 270 h of operation.

The addition of porous carbon materials to ZnO and alloying or electroplating with other metals have also proved to solve the challenges at the anode. For example, Deckenbach et al.[31] developed a 3D hierarchically porous ZnO/C nanoparticle anode material for RZABs. The ZnO/C material overcame the anode degradation by suppressing dendrite growth, Zn dissolution, and passivation. That is attributed to the

embedding of ZnO nanoparticles in the hierarchical porous carbon matrix results in maximized ionic and electron conductivities. The fabricated RZAB showed an improved Zn utilization, a peak discharge capacity of 267 mAh g^{-1} with stable capacity retention after 60 cycles. Similarly, a 3D Zn-entrained activated charcoal anode was reported by Okuwa et al.[32] that can alleviate the challenge of low output current density and increase the available surface area for anodic reactions. The fabricated RZAB using a 3D anode delivered a higher open-circuit voltage (OCV) than the conventional RZAB using planar anode. The fabricated RZAB was further proposed for higher power applications because the polarization test confirmed the high current density *ca.* 2.5 times higher than that of the RZAB using 2D planar anode. Wei *et al.*[33] reviewed previous reports on Zn metal challenges in an alkaline environment and used a non-alkaline electrolyte 1.0 mol kg^{-1} Zn(OTf)$_2$ to solve the electrochemical irreversibility. The fabricated Zn anode in 1.0 mol kg^{-1} Zn(OTf)$_2$ showed a distinct discharge plateau at ≈1.0 V and a real capacity of 52 mAh cm^{-2} (specific capacity of 684 mAh g^{-1}). In addition, the Zn anode in the non-alkaline electrolyte (1.0 mol kg^{-1} Zn(OTf)$_2$) had a Zn utilization ratio of 83.1%, which was higher than that in the alkaline electrolyte of 6.0 mol kg^{-1} KOH (8.1%). The Zn utilization ratio increased to 93.7% when Zn foil anode was replaced with Zn powder. Thus, this non-alkali ZAB allowed durable operations in ambient air and significantly better reversibility than its alkaline counterpart, attributed to (Zn^{2+})-rich inner Helmholtz layer on the air cathode originated by the hydrophobic (OTf) trifluoromethanesulfonate anions. Qu's group[34] electroplated Zn on Cu foam substrate to produce 3D Zn-coated foam anode for a flexible RZAB, which was further aided with polyvinyl alcohol (PVA)–tetraethylammonium hydroxide (TEAOH)-KOH hydrogel. The fabricated flexible semi-solid-state RZAB had an increased specific capacity and energy density of 566.7 mAh g^{-1} and 586.5 Wh kg^{-1}, respectively, and with high cycle stability. Similarly, Yu et al.[35] demonstrated that the Zn dendrite growth and corrosion could be effectively suppressed using Ag-modified 3D Zn anode in RZABs. The 3D anode reduced the zinc-air energy loss by improving the electrochemical kinetics and mass transfer. The electrochemical measurements (Tafel and linear scanning voltammetry) showed that the 3D anode had reduced HER and corrosion current. The fabricated RZAB had 94% coulombic efficiency after 80 cycles at a 2 h cycle period. The series and parallel connections of the two rechargeable batteries had high energy efficiencies of 55 and 60%, respectively, and stable cycling above 40 cycles. Kim et al.[36] proposed that the surface-modified Zn anode (i.e., modified with 0.1 wt.% CuO) showed increased reversibility and inhibited dendrite growth in RZABs, as shown in Figure 5.

The electrochemical results showed that the modification of the Zn anode surface effectively improves its properties, as the 0.1 wt.% CuO-modified Zn anode had a higher specific capacity (658.25 mAh g^{-1}, 26.33 cycles) than that of the bare Zn electrode (454 mAh g^{-1}, 18.33 cycles). Therefore, the modified Zn anode had increased corrosion inhibition effects, reversibility, and operation duration than the bare Zn anode. That was because the modified surface prevented the direct contact of

ChemElectroChem

Review
doi.org/10.1002/celc.202100574

Chemistry Europe
European Chemical
Societies Publishing

Table 1. Summary of the strategies for resolving the Zn anode challenges in RZABs.

Anode material	Challenges mitigated	Strategic method	Electrochemical performance	Refs
Zn−Bi mixed powders	Dendrite growth, passivation, HER, and corrosion	Combination of electrolyte additives BTA and TBAB	Increased specific capacity of 475.6 mAh g^{-1} relative to that without additives (327.3 mAh g^{-1}) and capacity retention of 83.2% after 50th cycles	[28]
Zn metal	Dendrite growth	Design of a novel multiphase alkaline electrolytes	The RZAB had energy densities of 196.2 Wh kg^{-1} and 309.1 Wh L^{-1} and outstanding capacity retention of 100% after 10,000 cycles at 50 mA cm^{-2}	[29]
Ionomer coated Zn anode	Zincate solubility, shape change, dendrite growth, and HER	Combined mitigation strategies (ionomer coating of the anode and electrolyte additives)	Increased specific energy (25 Wh kg$^{-1}_{Zn}$), cycle life, and battery roundtrip efficiency greater than 55% after 270 h	[30]
3D hierarchically porous ZnO/C nanoparticle	Dendrite growth, Zn dissolution, and anode passivation	Zn anode modification (The ZnO nanoparticle were embedded on hierarchically porous carbon matrix which maximized ionic and electrical conductivities)	Improved Zn utilization having a peak discharge capacity of 267 mAh g^{-1} with stable capacity retention during 60 cycles	[31]
3D Zn-entrained activated charcoal anode	low output current and rapid power loss	3D Zn-entrained anode	The 3D RZAB had a current density of ca. 2.5 times higher than that of the 2D planar RZAB	[32]
i. Zn foil ii. Zn powder	Electrochemical irreversibility	Use of a non-alkaline electrolyte 1.0 mol kg^{-1} Zn(OTf)$_2$	A distinct discharge plateau at ≈ 1.0 V, and a real capacity of 52 mAh cm^{-2} (specific capacity of 684 mAh g^{-1}). Zn utilization ratio of 83.1% and 93.7% when the Zn foil as an anode was replaced with Zn powder	[33]
3D porous structure electroplated Zn on Cu foam substrate	i. Dense morphologies with small effective surface areas and insufficient utilization of Zn ii. Poor contact between the Zn powder and current collector iii. The evaporation of the water in the electrolyte which lowers the ion-conduction and mechanical properties	i. Electroplating of Zn on Cu foam substrate ii. The use of semi-solid-state alkaline electrolyte (PVA-TEAOH-KOH hydrogel) has improved water retention ability.	Increased specific capacity of 566.7 mAh g^{-1}, the energy density of 586.5 Wh kg^{-1} with high circle stability (48 cycles, 32 h)	[34]
Ag-modified 3D Zn anode	Zn dendrite growth and corrosion	Ag-modified 3D Zn anode	94% coulombic efficiency after 80 cycles with 2 h cycle period. The series and parallel connections of the two batteries have a high energy efficiency of 55 and 60%, respectively and stable cycling at over 40 cycles	[35]
0.1 wt.% CuO-modified Zn anode	Dendrite growth, Zn reversibility and corrosion	Surface-modified Zn electrode	The 0.1% wt.% CuO-modified Zn anode has a higher specific capacity (658.25 mAh g^{-1}, 26.33 cycles) than the bare Zn electrode (454 mAh g^{-1}, 18.33 cycles)	[36]
KOH-treated silica-coated Zn particles	Zn passivation	KOH-treated silica-coated Zn particles	100% depth-of-discharge rechargeability, higher charge carrier numbers, and less electrochemical activation energy	[37]
ZBKP anode	Dendrite growth and HER	Anode additives	The ZBKP anode had the highest positive electrode potential	[39]
Electroplated Zn anode	Zn passivation and utilization	Fabrication of Zn anodes by electroplating processes	High specific capacity (711 mAh g^{-1}), battery efficiency (86.7%) and peak power density (23.4 mW cm^{-2})	[40]
i. Zn foil ii. Zn sponge doped In and Bi iii, Zn particles treated with In and Bi	The relationship between the HER and other anode reactions	Anode surface analysis, operando gas analysis and electrochemical measurements	The rate of HER was a function of applied current density and Zn anode surface area	[41]
Structured microporous Zn electrodes	Zn foil electrode's low surface area, ZnO layer passivation, and shape change during electrical recharging	Cost-effective production of structured microporous Zn electrodes	Outstanding cycle performance and Zn reversibility without substantial change in morphology, structure, and shape	[42]
Porous Zn anode	Zn reversibility and corrosion	higher surface area and number of active sites of Zn-001	The specific capacity of the porous Zn-001 (821 mAh g^{-1}) was higher than the pure Zn anode (418 mAh g^{-1})	[43]
Zn micro-spheres	Zn dendrite growth and Zn utilization	3D-printing technology	The high discharge capacity of 670 mAh g^{-1} at 5 mA cm^{-2} and high cycle stability after 350 cycles	[44]

the anode with the KOH electrolyte; thereby, the formation of Zn(OH)$_4^{2-}$ and ZnO was minimized. Schmid et al.[37] investigated the electrochemical performances of Zn particles which were coated with silica (SiO$_2$) by chemical solution deposition (CSD)

ChemElectroChem

Review
doi.org/10.1002/celc.202100574

Chemistry Europe
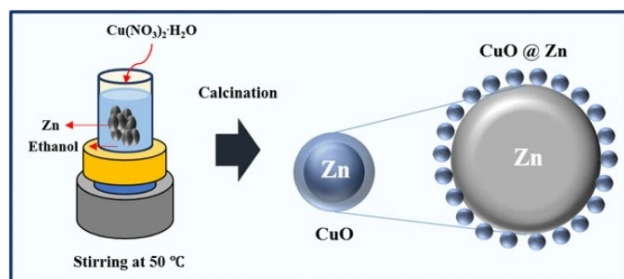European Chemical
Societies Publishing

Figure 5. Illustrating the synthesis process of CuO-modified Zn in Rechargeable zinc-air batteries. "Reproduced with permission from Ref. [36]. Copyright (2019) Elsevier".

and chemical vapour deposition (CVD), and subsequently treated in aqueous KOH. The results showed that the SiO_2 coated Zn particles have 100% depth-of-discharge rechargeability, higher charge carrier numbers, and less electrochemical activation energy than those without SiO_2 coating (both KOH treated). The Zn utilization of CSD-coated Zn anode, CVD-coated Zn anode, and the pristine zinc anode were 69, 62, and 57%, respectively.

Min et al.[38] used co-precipitation method to synthesize calcium zincate as RZABs' anode instead of the conventional Zn or ZnO. The calcium zincate anode showed high electrochemical reversibility because it was reduced to Zn and oxidized to $Zn(OH)_4^{2-}$ ions during charge and discharge processes, respectively. Herein, almost all the $Zn(OH)_4^{2-}$ ions can be converted to calcium zincate, resulting in a second cycle discharge capacity of 284 mAh g^{-1} and 96% coulombic efficiency. Aremu et al.[39] found out that among different Zn alloy anodes: ZBK (30 wt.% Zn: 3 wt.% bismuth oxide (Bi_2O_3): 10 wt.% potassium sulfide (K_2S)); ZBP (30 wt.% Zn: 3 wt.% Bi_2O_3: 5 wt.% lead (ii) oxide (PbO)) anodes; ZBKP (30 wt.% Zn: 3 wt.% Bi_2O_3: 10 wt.% K_2S: 5 wt.% PbO), the ZBKP showed the lowest dendrite growth and corrosion rate, using the electrolyte of 6.0 M KOH aqueous solutions with 1.88 wt.% polyacrylic acids. In addition, the ZBKP anode has the highest positive electrode potential relative to the other two anodes. Therefore, the ZBKP anode material adequately suppressed the HER and dendrite growth on the Zn anode's surface. Lin et al.[40] used the conventional direct current electroplating and pulse plating to fabricate the Zn anode. The results confirmed that the Zn anode produced by the electroplated process was more porous than the commercial Zn anode. Also, RZAB with electroplated Zn anode (PZn-500 Hz) had a specific capacity and efficiency of 711 mAh g^{-1} and 86.7%, respectively (i.e., 50% higher than the bulk Zn anode).

Morphology, structure, shape design, and 3D printing technology, are the recent strategies adopted for designing highly active and durable Zn anodes for RZABs. Dongmo et al.[41] used the electrochemical measurements, anode surface analysis, and operando gas analysis to reveal the relationship between the HER and other reactions at the anode. The results showed that the rate of HER was dependent on the applied current density and the Zn anode's surface roughness. These findings provided insight into the choice of optimal test

parameters and cell set-ups to achieve excellent RZABs' performances. A proof of concept study further confirmed the feasibility of the cold sintering process to synthesize porous Zn anode by Jayasayee et al.[42] The porous Zn anode shows outstanding cycle performance and Zn reversibility with insignificant changes in morphology and composition. Liu et al.,[43] compared the electrochemical performances of RZABs using porous Zn-001 and commercial pure Zn anodes. The porous Zn-001 had a higher initial voltage (1.33 V) than the pure Zn (1.26 V), signifying a higher reactivity. The specific capacity of the porous Zn-001 (821 mAh g^{-1}) was also significantly higher than that of the pure Zn anode (418 mAh g^{-1}), signifying a higher utilization ratio and energy efficiency for Zn-001. Also, the charge and discharge voltages of Zn-001 recorded were 1.96 and 1.33 V, while those of pure Zn were 2.28 and 1.26 V, respectively. Therefore, the Zn-001 had a lower charge-discharge difference (0.63 V) than pure Zn (1.02 V), attributed to the higher surface area/pores and the number of active sites of Zn-001 that facilitated faster electrochemical reaction kinetics and mass transport, which aided its outstanding reversibility and corrosion inhibition.

Zhang et al.[44] established a 3D-printing technology to produce both the anode and cathode for RZABs. The printed anode and self-standing air electrode are comprised of microsphere Zn and hierarchical porous cathode with high surface area, respectively. The micro-sphere anode afforded high Zn utilization that inhibited the Zn dendrite growth, while the hierarchical porous cathode offered high electrocatalytic activity and a fast diffusion-reaction channel. The RZAB had a high discharge capacity of 670 mAh g^{-1} at 5 mA cm^{-2} and high cycle stability after 350 cycles. Schmitt et al.[45] carried out multidimensional simulations of RZABs and validated the model with in-situ X-ray tomography of commercial RZABs. The results showed that the cycle life depends on the cell current and ZnO dissolution, and the best results were obtained for low charging currents.

3. The Air Electrode (Cathode)

The air electrode is perhaps the most significant part of the rechargeable RZABs, as it is responsible for the diffusion of O_2 from the atmosphere and drives its oxidation and regeneration. A typical air electrode comprises a gas diffusion layer (GDL), an electrocatalytic layer, and a current collector. The role of the GDL is to allow ionic transport, to ensure efficient oxygen diffusion from the air to the electrolyte, and prevent electrolyte flooding and leakage. The two distinct reactions (i.e., ORR and OER) take place at the air electrode.[46] The ORR (Equations (10) and (12)) occurs on discharge when the electrode is in contact with the ion-conducting electrolyte and the dissolved O_2.[2] The reversed process is the OER (Equations (11) and (13)) occurs during the charging process, which is the process of the O_2 regeneration through electrolysis of water, which is important to not only RZABs, but also several energy conversion and storage processes such as fuel cells, water splitting, amongst others.[47,48]

ChemElectroChem

Review
doi.org/10.1002/celc.202100574

**Chemistry
Europe**
European Chemical
Societies Publishing

3.1. Cathode Reactions Mechanism

The possible reactions at the cathode of rechargeable RZABs in an alkaline electrolyte are illustrated in Equations (10)–(13):[49]

Discharging process in alkaline electrolyte: Oxygen penetrates the porous cathode which reacts with water to produce hydroxide ions,

$$O_2 + 2H_2O + 4e^- \rightarrow 4OH^- \ (ORR, E^0 = 0.4\,V) \tag{10}$$

This process is ORR that occurs at the three-phase boundary i.e., the gas-solid-liquid phase inherent in hydrogen fuel cells. Where O_2 from the atmosphere (gas phase) diffuses through the GDL to the catalysts (solid phase), where it adsorbed and reduced to OH^- with its reaction with water and transferred to the electrolyte (liquid phase). ORR proceeds through two main routes: i) direct four-electron transfer pathway (Equation (11)) and two-electron pathway $(O_2 + H_2O + 2e^- \rightarrow OOH^- + OH^-)$, which is calculated by Koutecky–Levich (K–L) equation. A four-electron pathway is more favoured, whereas the two-electron pathway is more commonly used in mechanical H_2O_2 generation.
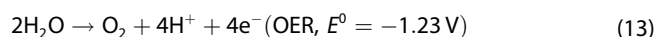
Charging process: Oxygen is regenerated from OH^- with e⁻s flow through the external circuit.

$$4OH^- \rightarrow O_2 + 2H_2O + 4e^- \ (OER, E^{0=}-0.4\,V) \tag{11}$$
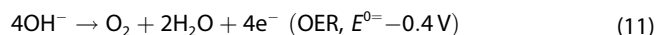
Discharging process in mildly acidic electrolyte: Here oxygen is reduced to water

$$O_2 + 4H^+ + 4e^- \rightarrow 2H_2O \ (ORR, E^{0=}1.23\,V) \tag{12}$$
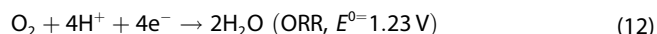
Charging process: During OER, water is oxidized to oxygen and hydrogen ions

$$2H_2O \rightarrow O_2 + 4H^+ + 4e^- (OER, E^0 = -1.23\,V) \tag{13}$$

The reaction processes in acidic media lead to the corrosion of zinc, morphology change, production of heat, and poor efficiency. Therefore, the overall reaction during the discharge/charge process when the anodic and cathodic reactions are combined as expressed in Equation (3) above.

Major challenges on the cathode side of RZABs are low efficiency because of the slow kinetics of ORR and OER with high overpotentials, necessitating the use of efficient bifunctional electrocatalysts. Moreover, the OER and ORR electrocatalysts are prone to degradation at high overpotentials. The electrocatalyst degradation could be traced to slow ions or electron transport, reduced active sites, poor structural stability, etc.[50,51] The RZABs also suffer from poor cyclability due to the high solubility of zincate ions from the anode, especially in alkaline conditions, which may permeate the separator and negatively affect the bifunctional air electrocatalysts. Furthermore, the continuous accumulation of insoluble ZnO in the electrolyte blocks O_2 transport channels to the air electrode and prevents further reactions. Therefore, low cell voltage (*ca.* 1.0 V) and poor power output are due to the inefficiency of the air

electrocatalysts. The air electrode deteriorates rapidly during charging because of the growth of O_2 bubbles and the corrosion of the air electrode.[52] Also, as much as the atmospheric air is of great importance in the operation of RZABs, it presents a challenge because carbon dioxide (CO_2) in the air may react with OH^- ions to form carbonate anions that poison the air electrocatalysts. Thus, there is a need to economically design the air electrode with low overpotentials, improved stability, recyclability, and cycle life.

3.2. Progress in Cathode Materials for Rechargeable Zinc-Air Batteries

Noble metals (e.g., Pt, Pd, Ru, and Ir) and their oxides respectively are the most active ORR and OER electrocatalysts.[53–56] For instance, Pt/C electrocatalyst shows excellent ORR activity at 284 mV, whereas RuO_2 displays great OER performance at 250 mV in 0.1 M KOH.[57] However, due to their scarcity, high cost, and self-poisoning, these materials are economically undesirable for the large-scale manufacturing of RZABs.[57] Thereby, various efforts have been dedicated to tailoring the shape, composition, and catalytic properties of noble metals electrocatalysts to enable high discharge power and energy densities with a minimal amount of noble metals. Another efficient approach is to replace noble-metal electrocatalysts with earth-abundant and low-cost catalysts like metal oxides (e.g., cobalt oxides, nickel-cobalt oxides, and manganese oxides),[58,59] metal chalcogenides (e.g., cobalt sulfides and nickel sulfides),[60,61] transition-metal-based molecular complexes (e.g., Co- and Ni-porphyrin complexes),[62] heteroatom-doped carbons (e.g., N, P, S, F and B),[63] M–N–C type materials (e.g., Fe–N–C and Co–N–C), mixtures of these various elements and allotropes of carbon-based materials..[64]

The RZABs have great resemblances to the OER and ORR processes of fuel cells.[48] Therefore, the successes of fuel cell technology are of great significance to the development of rechargeable RZABs. Amongst the major strategies is structural engineering or designing to modify, modulate and improve the performance of electrocatalysts toward ORR and OER.[65] Hence, Tomboc et al.[66] reported three modification strategies for the air cathode: (i) defect engineering; (ii) cation/anion regulation in multi-components transition metal compounds; and (iii) single or multi-heteroatom doping in carbon, as illustrated in Figure 6.

An air cathode must have dually coupled active sites to catalyze both OER and ORR activities, i.e., a bifunctional electrocatalyst for O_2 electrochemistry with the desired 4e⁻ ORR/OER pathway is favourable at low overpotentials, as shown in Figure 7.

In general, the active sites in electrocatalysts are designed to be dually functional towards ORR and OER or a monofunctional that catalyzes either ORR or OER.[55] Bifunctional air electrocatalysts are materials that have quantifiable activities for both the forward (ORR) and reverse reaction (OER).[70] The bifunctional air electrocatalysts effectively drive ORR and OER during discharging and charging concurrently such that there will be no need for having two electrocatalysts. These strategies
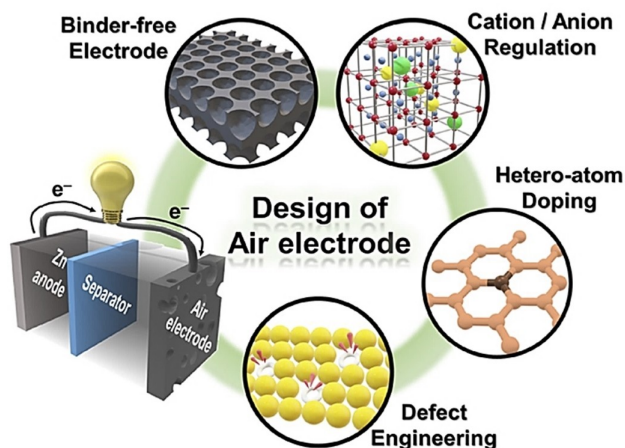
ChemElectroChem

Review
doi.org/10.1002/celc.202100574

**Chemistry
Europe**
European Chemical
Societies Publishing

Figure 6. Recent developments of the air electrode design for RZAB. Adapted with permission from Ref. [66]. Copyright (2020) The American Institute of Physics".

afford cost-effectiveness and enhance stability. There are cases where a particular electrocatalyst catalyzes one reaction more than the other, i.e., materials could be ORR active but OER less effective.[71,72] It was established that Pt and Fe/N/C are the state-of-the electrocatalysts for ORR, while Ni, Co, Mn, and Ru in perovskites are more active for OER.[73] However, carbon-based materials can be active toward ORR and OER in alkaline media, especially when structurally defected with nitrogen (N).[74] A three-dimensionally engineered N-doped graphene nanoribbons (N-GRW) containing electron-donating quaternary N-sites

and electron-withdrawing pyridinic N moieties that are active for ORR and OER, respectively, with excellent stability in alkaline media compared to noble electrocatalysts (Pt/C and Ir/C).[70] The nitrogen doping state was determined with the Mott-Schottky experiments. The n-type and p-type nitrogen were found for the quaternary and pyridinic N, respectively, and are the dominant components in the N-doped graphene catalyst. X-ray absorption near-edge structure (XANES) spectroscopic measurements were used to identify OER and ORR active sites. The electron-withdrawing pyridinic N moieties served as OER active sites, while the electron-donating quaternary N was responsible for ORR. The 3D structure provided high active sites and excellent mass and charge transport. The electrode material was then tested under tow-electrode that was loaded on a carbon cloth/gas diffusion layer. Before battery testing, the N-GRW-loaded carbon cloth hybrid electrode was tested in O_2-saturated 6 M KOH and had stability over 20 h of continuous OER/ORR cycles at $5 \, mA \, cm^{-2}$. The battery tested N-GRW at $20 \, mA \, cm^{-2}$ could produce charge/discharge current density at 1.09 and 2.18 V outperforming Pt/C (1.15 and 2.53 V) and Ir/C (0.95 and 2.07 V), but comparable to Pt/C+Ir/C (1.06 and 2.07 V) air electrode. During discharge, the normalized specific capacity at $2 \, mA \, cm^{-2}$ was $873 \, mAh \, g^{-1}$ with a peak power density of $65 \, mW \, cm^{-2}$ achieved over 150 cycles. The galvanostatic charge/discharge at $20 \, mA \, cm^{-2}$ in 6.0 M KOH and 0.2 M $ZnCl_2$ with good stability for 30 h of cycle time. However, the performance was affected by carbonate formation, which was corrected by replenishing the electrolyte and removing CO_2 regenerated, and maintained the battery stability and performance. Also, metal-N bonds have proved to be a crucial factor in
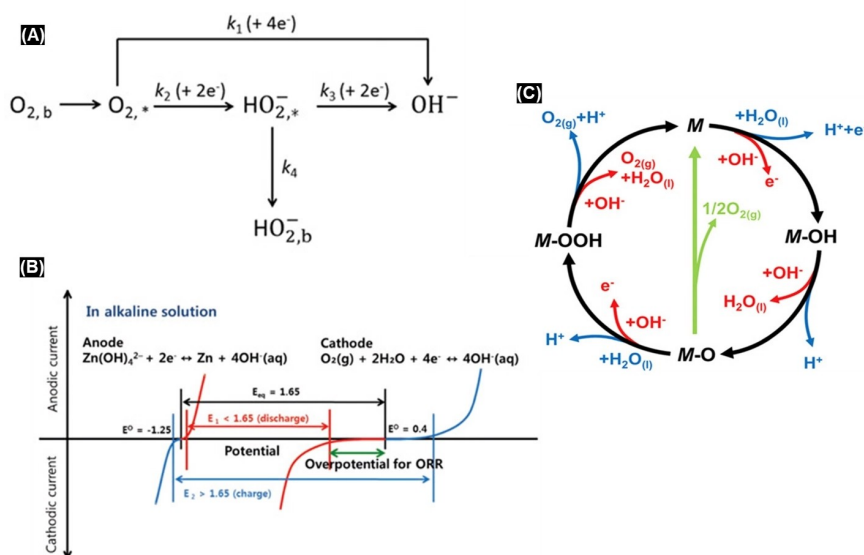

Figure 7. (A) Simplified ORR mechanism, illustrating the direct and indirect pathways with the associated phenomenological rate constants k_1, k_2, and k_3. Subscripts b and * designate bulk and reaction layer, respectively. "Reproduced with permission from Ref. [67]. Copyright (2016) Wiley-VCH". (B) Schematic polarization curves of RZAB cell with the equilibrium potential (black line) being 1.66 V, but the practical voltage (red line) in discharge is lower than 1.66 V due to the sluggish ORR. A large potential is required to charge RZAB, higher than the equilibrium potential (blue line). "Reproduced with permission from Ref. [68]. Copyright (2011) Wiley-VCH". (C) Schematic representation of OER mechanism in acid (blue line) and alkaline (red line) media, with the black line indicating that OER involves the formation of a peroxide (M−OOH) intermediate and/or other routes for the direct reaction of two adjacent oxo (M−O) intermediates (green) to generate oxygen. "Reproduced with permission from Ref. [63]. Copyright (2020) Wiley-VCH".

ChemElectroChem

Review
doi.org/10.1002/celc.202100574

**Chemistry
Europe**
European Chemical
Societies Publishing

enhancing the ORR and OER performances.[75] For example, Liang and co-workers[76] revealed that Co_3O_4/N-doped graphene hybrid (Co_3O_4/N-rmGO, ORR, $\sim$5.0 mA cm^{-2}) out-performed Co_3O_4/graphene (Co_3O_4/rmGO, ORR, $\sim$4.5 mA cm^{-2}) and Co_3O_4 due to the interfacial Co–N bonds between Co_3O_4 and N-doped graphene in 0.1 M KOH. The Co_3O_4/N-rmGO exhibited excellent stability in 0.1–6 M KOH compared to Pt/C (30% activity loss in 10 000s) and Pd/C (20% activity loss in 10 000s). Another study showed that pyridinic-N with strong Lewis basicity was the most active site for ORR and OER compared to the graphitic-N.[77]

Coupling graphene with transition metals or metal oxides such as perovskites and spinel could substantially enhance the ORR and OER performances relative to metals/oxides or graphene alone.[78] Hence, spinel or porous perovskite metal oxides have shown promising bifunctional electrocatalytic activities in alkaline solutions.[79–82] Perovskite oxides have good structural flexibility and stability, high oxygen kinetics, electrical conductivity, and oxygen capacity..[83]′ The mesoporous nano-fiber $PrBa_{0.5}Sr_{0.5}Co_{1.5}Fe_{0.5}O_{5+\delta}$ (PBSCF-NF) showed a small onset potential of (OER, 1.52 V) smaller than that of IrO_2 (OER, 1.56 V) in 0.1 M KOH, which showed a long-term cycling stability test (5000 cycles). Meanwhile ORR achieved 3000 cycles with 0.73 V onset potential in 0.1 M KOH and a well-maintained crystal structure. The ZAB set-up was performed in 6.0 M KOH, the battery at discharge current density of 10 mA cm^{-2} had a lower operating voltage and duration (1.25 V, 56000 s) than Pt/C (1.38 V, 48000 s). Retuerto et al.[73] investigated $La_{1.5}Sr_{0.5}NiMn_{0.5}Ru_{0.5}O_6$ (LS NMR) double perovskite for ORR and OER activities, which recorded the ORR onset potential ($E_{onset=}$ 0.83 V at 10 mA cm^{-2} for 200 cycles) and that of OER ($E_{onset=}$ 1.66 V at -1 mA cm^{-2} for 100 cycles). These values are pre-sumed to be amongst the best recently reported in alkaline media. The excellent ORR and OER performance of the double perovskite was attributed to the presence of Mn and Ru, respectively. Another study by Li and co-workers[77] reported that N-doped graphene has different chemical states of N ranging from pyridinic-N, graphitic-N to pyrrolic-N with enhanced ORR and OER activities. The need to maintain the ORR and OER activities after cycling at high potential, a study of core-corona structured bifunctional air electrocatalyst of N-doped carbon nanotubes (N-CNTs) (ORR active) and a core $LaNiO_3$ (OER active) was investigated.[84] The activity and stability of the bifunctional air electrocatalysts towards the O_2 electrochemistry were greatly maintained, thanks to the core-corona structure and the synergistic effect of the homogenous N-CNT to the core $LaNiO_3$. The current charge reported for the core-corona structured electrocatalyst was 1.5 times higher than Pt/C for half-cell studies. Charging and discharging of a single-cell test of the core-corona structured bifunctional air electrocatalyst conducted in 6.0 M KOH at 50 mA also outper-form Pt/C.[84]

Metal oxides have excellent ORR electroactivity but poor OER activity in alkaline medium.[6] Amongst the non-precious metal oxides, manganese dioxide (MnO_2) has been recognized as an attractive ORR candidate considering its rich oxidation states, crystalline nature, low cost, low toxicity, and environ-

mental friendliness.[58] However, MnO_2 has poor conductivity. One way to solve this issue is incorporating carbon to achieve improved electrical conductivity and high surface area. How-ever, the composites suffer agglomeration during pyrolysis, which possibly reduces the catalyst's efficiency and activity. However, the agglomeration of the composites derived from MOFs can be mitigated by acid treatment after pyrolysis.[85–87] Spinel metal oxides, on the other hand, have good ORR and ORR activities due to electron hopping between metals at different valence states, surface redox centres and high electro-catalytic activity.[88] Hierarchically 3D ordered mesoporous cobalt oxide (3DOM Co_3O_4) was investigated for OER and ORR activity for application as an air cathode in RZAB.[89] The bifunctionality of 3DOM Co_3O_4 was a result of the blended valences of coexisting cobalt cations facilitating electron move-ment by providing donor-acceptor chemisorption sites for both reversible oxygen adsorption and desorption in the cubic spinel structure.[89] The 3DOM Co_3O_4 (-0.197 and -0.360 V) had a more positive onset and half-wave potential than the bulk Co_3O_4 (-0.234 and -0.394 V). The ORR and OER Tafel slopes were lower for 3DOM Co_3O_4 (72 and 58 mV/decade) relative to bulk Co_3O_4 (84 and 90 mV/decade). 3DOM Co_3O_4 demonstrated high stability over 1000 cycles with just 13 mV voltage increase at 10 mA cm^{-1} and maintained morphology. Its ORR activity was slightly higher than the Pt/C and Ir/C composite but had comparable OER activity. To further test the air cathode material for the real application, an electrically RZAB was fabricated, the 3DOM Co_3O_4 had superior charge-discharge. Metal-organic frameworks (MOFs) are ideal templates to make composites that allow for an in-situ homogeneous dispersion of the metal and dopant within the porous carbon matrix with promoting charge transfer and more active sites.[90] Layered double hydroxide (LDH)-based materials are also promising air elec-trode materials. For examples, Gong's group[47] reported a NiFe LDH-CNT complex (NiFe-LDH/CNT) air electrocatalyst with high-er OER activity and stability than commercial Ir-based electro-catalysts with respect to lower E_{onset} and Tafel slope (b) but higher current densities, as well as improved stability after 1 h of operation.

In recent years, high-entropy alloys (HEAs) or metal oxides ($HEMO_x$) have also attracted great interest in oxygen catalysis due to their unique structural characteristics, tunable chemical compositions/properties, and relatively high reactivity. Many OER electrocatalysts have been reported, including high-entropy metal alloys,[91,92] high-entropy metal oxides,[93] high-entropy MOF,[94] high-entropy perovskite fluoride,[95] high-entropy metal glass.[96] In ORR, low Pt content or noble metal-free high-entropy alloys have been used as advanced ORR electrocatalysts, including AlNiCuPtPdAu[97] better than Pt/C in acid, AlCuNiPtMn[98] better than Pt/C in both acid and alkaline, CrMnFeCoNiMo and CrMnFeCoNiNb[99] in alkaline. Limited studies have been reported HEAs or HEMOx as bifunctional electrocatalysts for ORR and OER and/or applied in RZABs devices,[100,101] as shown in Figure 8. Recently, the Qui group[100,101] reported the use of multi-component nanoporous HEAs, i.e., AlNiCoFeCr[100] and nanoporous $HEMO_x$ of a spinel

ChemElectroChem

Review
doi.org/10.1002/celc.202100574

**Chemistry
Europe**
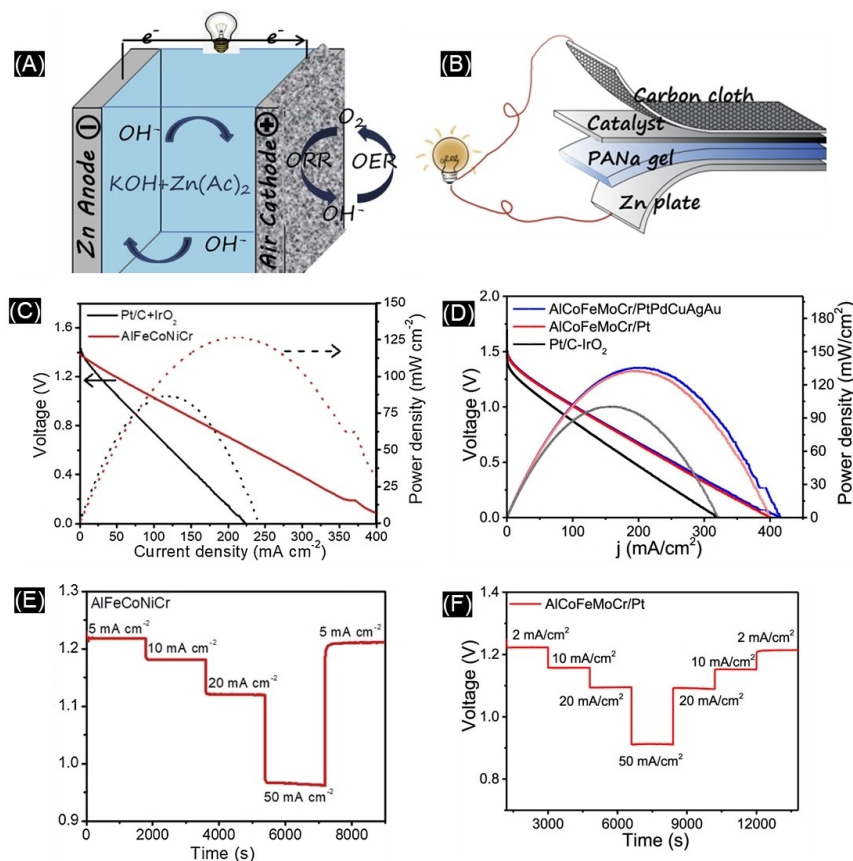European Chemical
Societies Publishing

Figure 8. Diagrammatic representations of (A) liquid RZAB (with a mixture of 6.0 M KOH and 0.2 M zinc acetate electrolyte) and (B) all-solid-state RZAB (with sodium polyacrylate (PANa) hydrogel electrolyte) using nanoporous AlFeCoNiCr electrocatalysts; Comparative polarization and power density curves of the liquid RZAB using either (C) AlFeCoNiCr or (D) AlCoFeMoCr/Pt; Comparative discharge voltage change with current densities and time for (E) AlFeCoNiCr and (F) AlCoFeMoCr/Pt. (A), (C), and (E) "Reproduced with permission from Ref. [100]. Copyright (2020) Elsevier; and (B), (D), and (F) Reproduced with permission from Ref. [101]. copyright (2021) American Chemical Society".

structure, modified with highly dispersed platinum nanoparticles (e.g., AlCoFeMoCr/Pt).

In both cases, the rich aluminum in the precursor intermediates (i.e., $Al_{97}Fe_{0.5}Co_{0.5}Ni_{1.5}Cr_{0.5}$[100] or $Al_{95.9}Co_1Fe_1Mo_1Cr_1Pt_{0.1}$[101]) serve as the sacrificial metal for the corrosion or etching process required to generate the desired nanoporous structures. In other words, the aluminum-rich intermediate alloy precursors that were obtained by extreme temperature melt method (i.e., 2650 °C under an argon atmosphere) and subjected to chemical dealloying/etching in 0.5 M NaOH solution to obtain the desired nanoporous HEA and HEMOx. Interestingly, although AlCoFeMoCr/Pt[101] showed better ORR activity than AlNiCoFeCr[100]), both alloys essentially gave the same electrochemical performance for RZAB (in terms of specific power density, energy density, and long-term cycling stability over the commercial Pt/C and Pt/C–IrO₂) despite the presence of a small amount of Pt in the former.

Morphology and size of the air electrocatalysts also play important roles in improving the OER and ORR activities. Nanostructured materials were reported to outperform micro-structured materials due to their high specific surface area.[102] For instance, Liu et al.[103] investigated tailored morphologies and sizes of Mn_3O_4: small nanoparticles (NP-S, 5.95 nm); large

nanoparticles (NP-L, 12.5 nm); nanoflakes (NF with Mn_3O_4 (101) exposure); and nanorod (NR with Mn_3O_4 (001) exposure). The NP-S Mn_3O_4 achieved 16.4 Ag_{ox}^{-1} at 0.83 V, which was the highest amongst the different morphologies. Similarly, Selvakumar et al.[104] developed engineered α-MnO₂ nanoparticles, nanowires (NW), and nanotubes (NT) as bifunctional OER and ORR electrocatalysts. The NW α-MnO₂ outperformed other electrocatalysts toward OER and ORR. Also, Pan's group[105] reported nanofibre α-MnO₂ as the cathode material in RZAB with over 5 000 cycles and 92 % retention capacity. Some other works that utilized non-noble metals-based bifunctional cathode materials in RZABs are summarized in Table 2.

4. Electrolytes

Unlike the Zn anode and air electrode in RZABs, electrolyte innovations have not generated much research interest. Meanwhile, the electrolytes have direct impacts on the ionic conductivity, interfacial properties, efficiency, and cycling stability of RZABs' operation.[52] Hence, developing highly efficient and durable RZABs is not only a function of the Zn anode and air electrode but also intertwined with the proper-

Table 2. Non-noble metal bifunctional electrocatalysts for air electrode in RZABs in terms of capacity (C), operating voltage (OV), electrolyte, power density (PD) and number of cycles (NOC).

Materials	C [mAh g^{-1}]	OV [V]	Electrolyte	PD [mW cm^{-2}]	NOC	Refs.
α-MnO$_2$ nanofiber	285.0	1.4	2.0 M ZnSO$_4$ /0.1 M MnSO$_4$	–	5000	[105]
Porous V$_2$O$_5$ nanofibers	319.0	0.5–1.5	3.0 M Zn(CF$_3$SO$_3$)$_2$	–	500	[106]
Co$_3$O$_4$@NCNMAs/CC ZIF-L-D-Co$_3$O$_4$/CC	815.0	1.5	6.0 M KOH/0.1 M Zn acetate	65.0	10000	[107]
NiCo$_2$O$_4$-CNT	636.0	1.4	6.0 M KOH	160.0	5000	[108]
Pd@3DOM-Co$_3$O$_4$		1.4	6.0 M KOH/0.2 M Zn acetate	–	300	[109]
a-MnO$_x$/TiC	769.8	0.7	6.0 M KOH/0.2 M Zn acetate	207.6	900	[110]
N-CoS$_2$ YSSs	744.0	1.41	6.0 M KOH/0.2 M Zn acetate	81.0	495	[111]
(Ni,Co)S$_2$	842.0	1.48	–	152.7	1440	[112]
Zn–Ni3FeN/NG	650.0	1.60	–	158.0	540	[113]
Cu–Co$_2$P@2D-NPC	736.8	1.40	6.0 M KOH/0.2 M ZnCl$_2$	236.1	480	[114]
NiIn$_2$S$_4$/CNFs	729.0	1.46	6.0 M KOH/0.2 M ZnCl$_2$	110	200	[115]
Ni$_{2.25}$Co$_{0.75}$N/NrGO	707.0	1.43	6.0 M KOH/0.2 M Zn acetate	193	500	[116]
Fe-NiNC-50	752.1	1.41	6.0 M KOH/0.2 M Zn acetate	220	600	[117]
CoDNG900	669.0	1.45	6.0 M KOH/0.2 M Zn acetate	205	2000	[118]
FeCoNi-NC	803.8	1.50	6.0 M KOH/0.2 M Zn acetate	315.2	100	[119]

ties of electrolytes.[120] On this note, research on the role of electrolytes in RZABs is of great significance with the view to understanding and improving the electrochemical performance of the emerging RZABs. Thus, it is imperative to note that the nature of electrolytes affects both the Zn anode and the air electrode of the RZABs, as elucidated below.

4.1. Fundamental Types of Electrolytes for RZABs

The electrolytes used in RZABs can be classified as (i) aqueous, (ii) non-aqueous, and (iii) solid-state electrolytes:

4.1.1. Aqueous Electrolytes in Rechargeable Zinc-Air Batteries

The Zn Pourbaix diagram (Figure 9) has revealed that Zn's reactions in aqueous media at equilibrium conditions are spontaneous, i.e., Zn is thermodynamically unstable in H$_2$O and other aqueous media because it tends to liberate H$_2$ via HER at varying pH ranges.[121] It is inferred that the electrochemistry of Zn tends to differ with respect to solutions' pH. This diagram highlights the instability of all surface oxides of Zn under acidic conditions due to its high solubility to form Zn^{2+} ions. Nevertheless, the possible formation of Zn oxide films in the pH range of 3.8–5.8, and the formed Zn oxide films tend to be porous and non-passivating.[121]

However, the solubility of Zn tends to decrease with increasing pH in acidic solutions, and under neutral or slightly alkaline conditions, the formation of more stable Zn corrosion
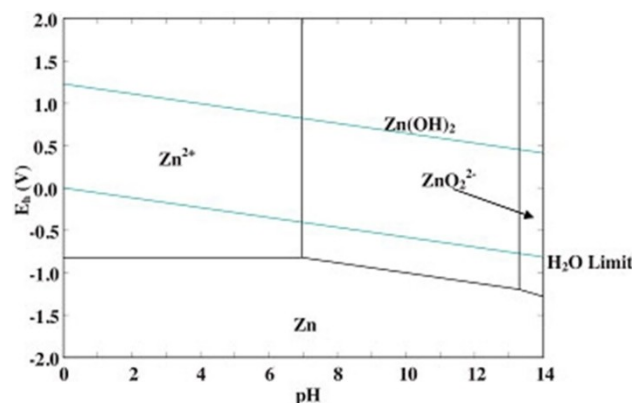
Figure 9. Zn Pourbaix diagram for reactions of Zn in aqueous media at 25 °C. "Reproduced with permission from Ref. [121]. Copyright (2014) Elsevier".

products (Zn(OH)$_2$) is enabled. At pH values higher than 9, i.e., more alkaline, the solubility of Zn increases with increasing pH favours the formation of insoluble ZnO$_2^{2-}$ because Zn(OH)$_2$ dissolves at this pH range. It is generally known that aqueous electrolytes are classified as: (i) alkaline, (ii) neutral, and (iii) acid.[122] The advantages and consequences of the aqueous electrolytes in RZABs are discussed extensively below:

Alkaline Electrolytes: Conventional RZAB utilizes aqueous alkaline electrolytes where both the Zn anode and air electrocatalysts are at their best conditions because it endears the following properties:[123–125] (i) electrochemical reversibility and fast kinetics of the Zn anode and air electrocatalysts for the ORR and OER; (ii) high ionic conductivity; (iii) relatively good performance at ambient temperature; (iv) high solubility of Zn

ChemElectroChem

Review
doi.org/10.1002/celc.202100574

Chemistry
Europe
European Chemical
Societies Publishing

salts; and (v) possibility of using non-Pt, economically effective and durable positive electrodes. Thus, the most commonly used electrolytes in RZABs are alkaline aqueous solutions containing potassium hydroxide (KOH),[121] sodium hydroxide (NaOH),[126] and lithium hydroxide (LiOH).[127] The KOH solution is the most preferred and extensively used electrolyte because of its fast electrochemical kinetics and high solubility of Zn salts, coupled with the superior ionic conductivity of K^+ (73.50 Ω^{-1} cm^2 equiv^{-1}) compared to Na$^+$ (50.11 Ω^{-1} cm^2 equiv^{-1}).[128]

Neutral Electrolytes: In recent years, interest in neutral electrolytes for RZABs have increased due to the principal advantages of neutral electrolytes when compared to alkaline media:[129] (i) it avoids the carbonization of the electrolyte that may poison the air electrocatalysts; and (ii) minimizes dendrite formation of the Zn anode. Because in neutral pH of the electrolyte, there is reduced Zn solubility and eliminated CO_2 absorption. The tuning of the electrolyte to around pH 7 can be achieved with solutions such as KCl, KNO_3, Na_2SO_4, and K_2SO_4 or to around pH 5 using ammonium salts, and the latter electrolyte is regarded as near neutral when compared to acidic or alkaline solutions prepared using H_2SO_4 or KOH, respectively.[130] However, Zn could only dissolve in neutral electrolytes containing anionic species (like Cl$^-$ ions) that are non-reducible by Zn.

Acidic Electrolytes: The use of acidic electrolytes in RZABs has been slowed down by the need to find a suitable electrocatalyst capable of overcoming the inherent problems associated with the air electrocatalyst's poor activities and low life span at the air electrode, as well as ease of corrosion of the Zn anode. Examples of acidic electrolytes include H_2SO_4, H_3PO_4, HNO_3, and HCl acids. In acidic electrolytes, the electrochemical behaviour is different from that of alkaline electrolytes, as the rate at which dendrite formation proceed is higher than that of alkaline electrolytes. Also, the passivation of Zn's surface by the evolved H_2 does occur fast in acidic than alkaline solutions, though the mechanism of dissolution to form complex and non-complex solutions differs.

The challenges of RZABs that utilize aqueous electrolytes include:[131] (i) water evaporation or ambient moisture uptake; (ii) bicarbonate formation; (iii) limited electrochemical window leading to poor cell behaviour or difficulty in being recharged due to the difference between the OCV and stability window of aqueous electrolytes between 1.23 V and 1.65 V; and (iv) short battery shell-life.

4.1.2. Non-Aqueous Electrolytes in Rechargeable Zinc-Air Batteries

These problems associated with the aqueous electrolytes have increased research interest to investigate alternative electrolyte systems. Thus, the use of non-aqueous electrolytes is emerging with efforts to properly gain insights into their solvation and electrochemical properties as potential candidates in RZABs. The major non-aqueous electrolytes are organic compounds. The organic electrolytes can offset a number of the challenges associated with RZABs that use aqueous electrolytes. Organic electrolytes can prevent side reaction that evolves H_2 gas,

mitigate dendrite formation, dry-out of the electrolyte from water evaporation and carbonation.[132] These non-aqueous electrolytes have characteristic high thermal stability and can operate at a wide potential window. However, the following problems such as volatility, flammability, and toxicity, are associated with non-aqueous electrolytes in RZABs. These fences could be overcome by ensuring appropriate compositions of organic solvents are used.[131,132] Although extensive research work has been carried out using organic electrolytes in lithium-ion batteries, such works in RZABs are still in infancy, notwithstanding few reports showed that non-aqueous electrolytes were promising for RZABs.[133,134] Although the mechanism of Zn dissolution is similar in both non-aqueous and aqueous solutions, the stabilities of monovalent cations and adsorbed intermediate species are much better in organic electrolytes. Therefore, the solubility of corrosive products is lower in organic solutions compared to aqueous media. The stability of surface species and the dissolution mechanism play vital roles in the electrochemical processes occurring on Zn anode and air electrodes in organic environments.[133,134]

4.1.3. Solid-State Electrolytes in Rechargeable Zinc-Air Batteries

The solid-state electrolytes explored so far mainly include *solid-polymer electrolytes (SPEs) and gel-polymer electrolytes (GPEs)*. The SPEs or thin-film electrolytes are ionic conductive solids macromolecules with heteroatoms that enable the dissolution of several salts and their diffusion when an electric field is applied.[127] The SPEs offer several advantages over current aqueous electrolytes in RZABs such as (i) good mechanical strength and potential ability to deform; (ii) ease in handling and enabling the formation of thin-films; (ii) reduced electrode corrosion and increased battery life due to low convention; and (iv) problem associated with battery leakage is eliminated. These advantages enhance the energy, operating temperature range, battery shell-life, and electrical rechargeability of the RZABs.[127] The main problems associated with the SPEs are: (i) their low ionic conductivity, not exceeding 1 μS cm^{-1} under ambient conditions;[135] (ii) low solubility of Zn salts; and (iii) formation of passive layers between the SPEs and the electrodes' surface;[127] (iv) high interfacial resistance to flow of OH$^-$ due to poor wetting property of the immobilized electrolyte.[136] In aqueous systems, the three-phase reaction zones consisting of *'solid (catalyst)-liquid (electrolyte)-gas (O$_2$)'* have full access to the electrolyte and facilitated faster transport of OH$^-$ ions compared to the solid configuration.[137] The high interfacial resistance led to low current rates and high overpotentials when the battery was in operation.

An important property of non-aqueous solid-state electrolytes is their adhesion to electrodes' surface when changes in volume occur during charging and discharging. Several SPEs have been reported in the literature, but the most widely studied are: poly(ethylene oxide) (PEO)-based electrolytes like PEO-ZnX$_2$ (where X=Cl, Br, I, ClO$_4$ and CF$_3$SO$_4$);[137] and PVA-proton/iodide systems,[138] as well as their combinations with Zn salts. The PVA-proton/iodide systems prevent Zn anode

ChemElectroChem

Review
doi.org/10.1002/celc.202100574

Chemistry
Europe
European Chemical
Societies Publishing

corrosion but are not suitable for RZABs applications due to their low conductivities.

The GPEs are formed when liquid electrolytes are sandwiched in a polymer gel to enhance the ionic conductivity of the electrolyte in the range of 10^{-4} to 10^{-3} S cm^{-1} at ambient temperature, making GPEs a good electrolyte for RZABs applications.[139] GPEs can generally be fabricated by a phase-inversion method that is preceded by immersion in liquid electrolytes, solvent casting steps, and the in-situ polymerization step.[139] In the fabrication of various polymers like PEO, poly(methyl methacrylate) (PMMA), poly(acrylonitrile) (PAN), and poly(vinylidene fluoride) (PVDF), different polymer matrices were used with aprotic solvents, including propylene carbonate (PC), ethylene carbonate (EC) and dimethylsulfoxide (DMSO).[140] For instance, Ikeda and co-workers[141] investigated a GPE composed of PAN and Zn triflate (Zn(CF$_3$SO$_3$)$_2$), which yielded a conductivity of 2.67×10^{-3} S cm^{-1} at room temperature. When the PAN was substituted with PVDF, a maximum ionic conductivity of 3.94×10^{-3} S cm^{-1} was obtained at ambient temperature.

4.1.4. Other Possible Electrolytes for Rechargeable Zinc-Air Batteries

Other possible electrolytes that have been used in RZABs are room temperature ionic liquids (RTILs) and deep eutectic solvents (DESs) which are discussed below: The RTILs are composed of organic cations and inorganic anions with interesting properties such as high electrochemical and thermal stabilities, low vapour pressure and flammability, make them attractive in RZABs.[142] Studies have shown that cations and anions can be fine-tuned to control their solvation properties and improve electrochemistry and eliminate the growth of dendrites on the Zn anode.[142,143] Highly concentrated RTILs electrolytes are known for their ability to enhance mass transport, thereby improving overall performance in RZABs.[144] The RTILs can also serve as additives to the Zn anode to increase the efficiency and durability of RZABs.[142–144] For example, Ghazvini et al.[145] reported the formation of electroactive Zn species at high concentrations of Zn acetate (ZnOAc)$_2$) ($>$4.0 M) with an RTIL (I-ethyl-3-methylimidazolium acetate (C$_2$mim)(OAc)) additive to facilitate Zn deposition/stripping. However, the drawback was that the electrochemistry was carried out at a high temperature due to the high viscosity of the high concentrations of the RTILs. The studies further showed that Zn reduction and oxidation could be achieved at room temperature by the addition of $\geq$ 20 vol % water to 1.0 M Zn(OAc)$_2$/[C$_2$mim][OAc], allowing water molecules to solvate both Zn^{2+} and acetate anions. Spectroscopic analysis using Raman, IR, and NMR justified that water addition created a hydrogen-bonded network with acetate anions, thereby disrupting and weakening the coordination of Zn^{2+} with (OAc)$^-$ ions and creates a new electroactive Zn^{2+} species.

The DESs are mixtures of solvents composed of Bronsted acids and bases joined via a hydrogen bond. Various types of DESs have been studied as potential alternative electrolytes for electrochemical applications in RZABs due to their low cost and environmentally benign nature.[146] The DESs also possess high ionic character and are highly polarized, i.e., they can easily dissolve high concentrations of various metal salts.[147] DESs mixtures containing chloride and urea are known to dissolve larger concentrations of ZnCl$_2$ than others leading to improved Zn deposition/stripping.[146,147] However, chloro-zincates are highly corrosive and have low oxidative stability resulting in a high voltage of RZABs. Qiu et al.[148] studied a DES containing Zn complex (([ZnTFSIm (Ace)n]$^{(2-m)}$ (m = 1–2, n = 1–3) using acetamide and Zn[TFSI]$_2$. The DESs were probed with Raman, FTIR, High-resolution mass spectrometry (HRMS), and Density Functional Theory (DFT) calculations. The results revealed that ions in the TFSI formed associative networks that decomposed before Zn deposition, forming a Zn-comparable solid-electrolyte interface (SEI) layer comprising ZnF$_2$-based organic products. The SEI layer formation was vital in producing dendrite-free, stable Zn cycling at the anode ($>$ 2000 cycles, CE = 99.7 %). The formation of the SEI layer opened a new pathway to modifying the Zn anode to improve the performance of RZABs.

The Comparison of the advantages and disadvantages of the different classes of electrolytes used in RZABs are summarized in Table 3.

4.2. Recent Progress in Electrolytes for Rechargeable Zinc-Air Batteries

The most common electrolytes used in RZABs are aqueous alkaline electrolytes; however, they are plagued by adverse factors, including Zn dissolution, Zn corrosion, shape changes, dendrite formation, precipitation of insoluble carbonates, electrolyte evaporation, and H$_2$ evolution.[123]

The high solubility of Zn in strong alkaline media leads to the precipitation of saturated or supersaturated zincate solution (Zn(OH)$_4$$^{2-}$) that is directly linked to dendrite formation and shape-changes and decreased the RZABs performance. Nevertheless, Zn(OH)$_4$$^{2-}$ species determines the electromotive force of the electrode.[62] Factors such as scan rate, Zn anode position and accessible water near the surface could also control Zn intermediate species' concentration.

The formation of passivating film layer that inactivates the Zn's surface occurs when the dissolution of the Zn induces excess solubility of the solid Zn or its hydroxides in the electrolyte within the vicinity of the electrode's surface.[149] This could decrease the discharge capacity and power capability of the Zn anode due to the passivating films being a barrier to the diffusion of OH$^-$ ions. The use of highly concentrated alkaline solutions can reduce Zn passivation by dissolving the passivating films. However, at high solubility, this mitigation strategy can induce shape changes. The use of additives such as silicate (SiO$_3$$^{2-}$) in the electrolyte modifies the electrode's surface and suppresses the blocking effect of the passivating layer on the diffusion of discharged Zn^{2+} ions.[150] Surfactant sodium benzene sulfonate (SDBS) in an alkaline electrolyte, especially at dilute concentrations, can also mitigate the Zn passivation and improve the Zn anode's discharge capacity.[151] The Zn passiva-

ChemElectroChem

Review
doi.org/10.1002/celc.202100574

Chemistry Europe
European Chemical
Societies Publishing

Table 3. Comparison of the advantages and disadvantages of different classes of electrolytes used in RZABs.

Electrolytes	Advantages	Disadvantages
(I) Aqueous (a) Alkaline	Electrochemical stability and fast kinetics of O_2 electro-chemistry. High ionic conductivity. Excellent performance at room temperature. High solubility of Zn salts. Possibility of non-Pt, economical and active positive electrodes.	Dendrite formation, shape change and H_2 evolution at the Zn anode. Leakages of the electrolyte. Safety issue.
(b) Neutral electrolytes	No carbonate formation in the electrolyte that may poison the bifunctional electrocatalysts and corrode the Zn anode. Reduce dendrite formation of the Zn anode and no H_2 evolution occurrence. Larger working potentials, safer and more robust alternative to alkaline.	Reduced solubility and activity of Zn anode. Considerably slower O_2 electrochemistry. Poor rechargeable ZAB performance.
(c) Acidic	High solubility of Zn. The oxide films of Zn formed are not passivating.	Poor bifunctional electrocatalysts' performance and low life span. Mandatory use of Pt-based electrocatalysts for optimum performance making the RZAB expensive. Ease of corrosion of Zn anode and bifunctional electrocatalysts.
(II) Non-Aqueous	Prevent H_2 evolution, mitigate dendrite formation, dry-out of electrolyte from water evaporation and carbonation. Operate at a wide potential window.	High volatility, flammability and toxicity. Low electrical conductivity.
(III) Solid-State	Good mechanical strength and potential ability to deform. Ease in handling and enabling the formation of thin films. Reduced electrode corrosion and increased battery life due to low convention. A problem associated with battery leakage is eliminated.	Low ionic conductivity, not exceeding 1 μS cm^{-1} under ambient conditions. Low solubility of Zn salts. Formation of passive layers between the solid-state electrolyte and the electrodes' surface. High interfacial resistance to flow of OH$^-$ due to poor wetting property of the immobilized electrolyte.
(VI) Other Possible (a) Electrolytes room temperature ionic liquids (RTILs)	High electrochemical and thermal stabilities. Low vapour pressure at room temperature. Controlled solvation properties and improved electrochemistry. Eliminate the growth of dendrites on the Zn anode. Ability to enhance mass transport.	Electrochemistry could only be carried out at a high temperature due to high viscosity. Disrupt and weaken the coordination of Zn^{2+} with (OAc)$^-$ ions.
(b) Deep eutectic solvents (DESs)	Low cost and environmentally benign nature. High ionic character and polarized. Improved Zn deposition/stripping	Highly corrosive. Low oxidative stability

tion occurs mainly at a high discharge scan rate; hence, using a slow scan rate suppresses the passivation. At this condition, more time is given for the cathode scan results in the dissolution of a large amount of the passivating layer.[151]

Shape changes and growth of dendrites are due to the high solubility of Zn. In alkaline RZABs, shape changes occur when Zn particles migrate owing to the gravitational pull from the top and side to the bottom.[125] The redistribution of active materials causes an irreversible loss of capacity and triggers the formation of dendrites, which can puncture the separators leading to an internal short circuit.[125] Zn anode's shape change and dendrite formation can be mitigated by adding compounds that suppress Zn dissolution in alkaline media.[152] The additives can form insoluble complexes with Zn and cause a reduction in the electrolyte's pH. Such compounds contain fluoride (KF), borate (K_3BO_3), phosphate (K_3PO_4), arsenate (K_3AsO_4), and carbonate (K_2CO_3), as well as electrolytes containing organic-inorganic compounds such as CH_3OH-KOH, could be used or the use of surfactants which have proven to inhibit the growth of Zn dendrites by controlling electrode passivation.[151,152]

Precipitation of insoluble carbonates occurs when the OH$^-$ ions in the alkaline electrolyte of RZABs react with carbon

dioxide in the air, forming carbonate (HCO$_3^-$) or bicarbonate anions (CO$_3^{2-}$). The carbonation process originates from several factors such as:[153] (i) reduction in ionic conductivity due to slower mobility of HCO$_3^-$ or CO$_3^{2-}$ in alkaline media; (ii) blockage of micropore in the air electrode due to low solubility of carbonates, impeding O_2 access with resultant reduction in air electrocatalyst's performance; (iii) a rise in electrolyte viscosity complicates O_2 diffusion into the electrolyte, which adversely affects the bifunctional air electrocatalyst for ORR and OER. Filters made up of CO_2 absorbents through chemical and/or physical absorption could be used to mitigate CO_2 absorption from the air. For example, Drillet's group[154] reported the removal of CO_2 from a feed gas in alkaline RZABs employing adsorbents based on physisorption and chemisorption processes (LiOH and LiOH-Ca(OH)$_2$). In another study, Cheng et al.[155] employed a chemisorption process that involves piperazine, 2-(2-aminoethylamino) ethanol, and monoethanolamine. The primary or secondary amine group of the compounds reacts actively with CO_2. Another approach was the incorporation of potassium carbonate (K_2CO_3) into the electrolyte with the potential of reducing the kinetics of carbonation species.[156] In this regard, Schröder et al.[157] reported that the addition of

ChemElectroChem

Review
doi.org/10.1002/celc.202100574

Chemistry Europe
European Chemical
Societies Publishing

approximately 30% mol K_2CO_3 to high molar KOH electrolyte led to an improved lifetime of the RZABs, though at a marginal battery performance loss.

In aqueous RZABs, evaporative water loss and ambient water uptake lead to long-term failure. Ambient water uptake in a high humid environment induces air electrode flooding and affects O_2 transport to the air electrocatalysts' active sites that also cause dilution of the electrolyte and subsequent reduction in the ionic conductivity over time with resultant higher internal resistances. Conversely, evaporative water loss increases electrolyte concentration, negatively affecting the discharge reaction.[158] To mitigate the effect of water, the electrolyte's volume and composition, the amount of Zn, gas diffusion degree and suitable battery design need to be optimized.[158] This study further elucidated that modification of electrolytes through polymerization, trapping of water, and a siloxane membrane method are the best approaches employed to protect against dry out and flooding.

The simultaneous HER at the Zn anode's surface and water electrolysis (i.e., OER) at the air electrode during RZABs' charging cause a build-up of internal pressure. The HER as a side reaction leads to a decrease in the cycle life of RZABs and affects its capacity retention over the long term (i.e., ease of Zn anode corrosion).[157,158] During the Zn corrosion process, two simultaneous reactions occur at the Zn anode's surface. The Zn corrosion is the cathodic controlled reaction. Therefore controlling the cathodic HER limits significantly the rate of Zn corrosion. K. Wippermann et al.[159] demonstrated with a Pourbaix diagram that Zn/H_2O with Zn^{2+} in the electrolyte and ZnO as the solid product has the potential where the HER occurs at a current density of $-1.0\,mA\,cm^{-2}$. The studies reported that when the pH is greater than 12, i.e., it becomes more alkaline, the potential is higher than -1.6 V *vs.* SHE, then a high cathodic overpotential for the HER is observed. In another study, Thomas and co-workers[160] investigated Zn corrosion as a function of pH. In the pH range (1 to 4), the HER kinetics predominates the overall Zn corrosion rates. The pH range (4 to 11) revealed no significant change in Zn corrosion rate, due to a change from HER to ORR in the cathodic reaction. Whereas between pH range (11 and 12), a protective Zn oxide layer was formed, and the electrode potential was at -1.15 V *vs.* SHE, at these conditions, the Zn corrosion rate was minimized. To delay the HER, additives such as lead (Pb), antimony (Sb), bismuth (Bi), cadmium (Cd), and gallium (Ga) were incorporated into the electrolyte, but these make them impractical.[161] Alternatively, organic compounds as surfactants were used. Lee et al.[162] investigated ZnO anodes in the presence of phosphoric acid, tartaric acid, succinic acid and citric acid as additives to the alkaline electrolyte solution. An increase in the hydrogen overpotential of the ZnO electrode was induced by these organic acids, due to the partial covering of the Zn anode's surface by absorbed molecules and the active sites were blocked during cathodic polarization. The study revealed that though molecules with high polar groups minimize dendrite formation and HER, molecules with the least number of polar groups are very effective. This study further showed that when ZnO was added to the alkaline electrolyte, it

reduced the activity of water and consequently the HER. Suppression of water minimizes the solubility of zincate ions, but promotes the formation of ZnO, as well as the active material in the environment of the electrode surface, thereby preserving the morphology of the electrode and enhancing rechargeability.

5. Summary and Outlook

The availability of the RZABs in the market is limited by the challenges that span the Zn anode, air cathode / bifunctional electrocatalysts to electrolytes. Tremendous efforts geared toward addressing these challenges have been discussed. The zinc anode is conspired by four performance-limiting inter-related events, namely: dendrite growth, shape-change, passivation, and hydrogen evolution reaction. Dendrite growth and shape change can lead to short-circuiting, poor cell efficiency, and general battery life. To mitigate these challenges, it is recommended that research should focus on re-designing efficient zinc anode materials and/or use new electrolytes (e.g., polymer gel electrolytes) or additives to the electrolytes. Passivation is due to the insulating ZnO film on the Zn surface, resulting in several performance-limiting events such as internal resistance of the anode, voltage loss during charge-discharge cycles, decreased utilization of zinc anode, and poor capacity generation. It is strongly recommended that RZAB be re-design with efforts to improve zinc utilization. HER is an energetically favoured activity at the zinc anode (especially with ZnO-covered surface), thereby allowing corrosion to occur even when RZAB is at rest (self-discharge). One of the mitigating strategies that should be considered is coating the zinc anode with corrosion inhibitors that will not compromise the performance of the RZAB. One of such corrosion inhibitors may be found in zinc-based macrocyclic complexes such as the zinc phthalocyanine complexes.[163]

The development of novel bifunctional electrocatalysts is extremely important to mitigate the sluggish kinetics of oxygen reactions (ORR and OER). Although the expensive platinum group metals (PGMs) significantly improve the kinetics of ORR, they are extremely poor for OER, thus making PGM-based electrocatalysts unsuitable as bifunctional electrocatalysts for practical applications. Interestingly, however, several non-precious metal bifunctional electrocatalysts (including transition metals and metal-free carbon materials with low-cost and abundant mineral resources) can be designed with principles such as structural defect engineering, morphology and size control, heteroatom doping with unique features like high porosity and surface area, high electrical conductivity and thermal stability, oxygen vacancies or defect. In fact, several electrocatalysts have been proven to compete favourably with PGM-based electrocatalysts for ORR.[164–168]

The RZABs' anode and bifunctional electrocatalyst materials should be flexible and lightweight to adapt to space-saving integrations and miniaturization.[169] Rational design and modulation of the electrode materials would be a great deal to prevent agglomeration of bifunctional air electrocatalysts, poor

ChemElectroChem

Review
doi.org/10.1002/celc.202100574

Chemistry Europe
European Chemical
Societies Publishing

utilization of Zn anode and electrolyte poisoning, which can eventually lead to excellent battery efficiency and stability. The structural engineering and modelling of the Zn anode are needed to holistically offer lasting solutions to all the RZAB components' challenges. Also, growing the bifunctional air electrocatalyst directly on the GDL of the air electrode of RZAB could reduce contact resistance and facilitate mass and electron transports.[63]

The GDL used on the air electrode should have balanced water-repelling (hydrophobic) and water-retaining (hydrophilic) properties to allow oxygen diffusion with an efficient three-phase boundary for ORR and OER to perform at its optimal level and sustain high current density.[46] A recent and promising optimization strategy adopted for air electrodes in RZABs was the use of solar-assisted bifunctional air electrocatalysts that utilized solar or photo-radiation captured in a p-n junction to minimize the ORR and OER overpotentials, thus improve the energy efficiency during discharging and charging processes, respectively.[170,171] For instance, Figure 10a shows the solar-promoted RZAB with highly efficient air photoelectrodes (i.e., $BiVO_4$ and α-Fe_2O_3) having lowered overpotentials of -1.20 and -1.43 V, respectively. Figure 10b reveals the proposed mechanism of the air photoelectrodes toward the O_2 electrochemistry.[171]

The Zn anode should be designed for realizing optimal utilization and mitigating corrosion and passivation to barely minimum level. The choice of electrolyte prevents the dissolution of Zn and improves the RZABs' performances and durability, which are important factors used to determine the battery life cycle.

Since the RZABs are receiving so much attention recently, studies on parameters and performance descriptors are necessary for researchers to have a common platform for comparison.[3] That will help to improve the batteries' performance and provides much-needed knowledge in the field. The success of RZABs lies in the efficient and long-term battery

operation, with respect to stable Zn anode, bifunctional air electrocatalysts' reversibility and stability, as well as a good GDL. Also, the integration of novel materials like MXene-based, carbon-dots, graphdiyne, high entropy alloys, and carbon nitride materials with their unique physiochemical properties, catalytic merits, and Zn can enhance the activity and durability of RZABs. Meanwhile, various theoretical studies are needed to tailor the performance of RZABs and understand their mechanism.

The intriguing characteristics of RZABs with excellent theoretical energy and volumetric energy density, environmental benignity and economy made them one of the most promising energy systems to meet the huge demand in various applications, especially electric vehicle (EV) technologies. The great prospects of the RZABs informed its much attention amidst other energy storage systems. In the last decade, enormous efforts were dedicated to identifying its challenges and proffer lasting solutions to put forth the RZABs as a leading energy storage system in the global market. The commercialization of the RZABs is limited with its low energy efficiency and short life span, attributed to the irreversibility and instability of its major components: Zn anode, bifunctional air electrocatalysts, and electrolytes. Thus, major concerns of designing highly efficient and durable RZABs are directed to resolve the challenges occurring at Zn anode, air electrodes, and electrolytes, as discussed extensively in this study. Zn-based active materials have proved to mitigate the Zn dendrite growth, shape change, passivation, and H_2 evolution, thereby preventing capacity loss during discharging and charging processes. While at the air electrode, promising economic transition metals-based and carbon-based bifunctional air electrocatalyst materials are active toward O_2 electrochemistry (i.e., ORR and OER) with reduced voltage polarization during discharging and charging processes in RZABs. Recent efforts to substantially improve the RZABs' performances focus on air electrode
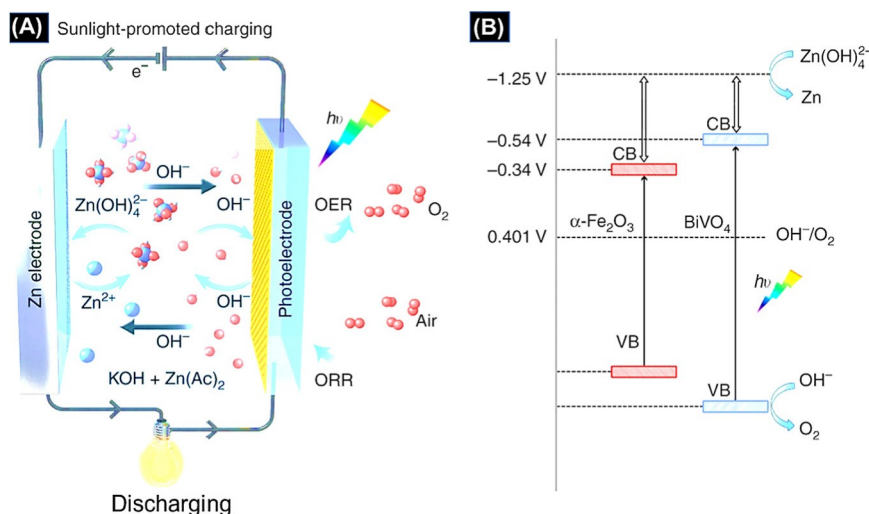

Figure 10. Schematic solar-promoted charge and discharge processes of solar-promoted RZAB. (A) The scheme working principle of the solar-promoted RZAB and (B) The proposed mechanism of the solar-promoted charging process under solar illumination. "Reproduced with permission from Ref. [171]. Copyright (2019) Nature Research".

material such as solar-induced and high entropy alloys bifunctional air electrocatalysts.

The type and composition of electrolytes have a significant effect on determining the performance of RZABs. The Zn anode and air electrode are ineffective in the aqueous alkaline electrolytes, due to their high tendency to carbonation in air. However, electrolyte additives with very strong adsorption for CO_2 can help to resolve the problems holistically. New electrolyte systems show great promises, including neutral aqueous, organic, ionic liquid-based, and DES electrolytes and this direction should be explored in the future. This review focused on the "static" RZAB rather than the "flow" system, i.e., rechargeable zinc-air flow batteries, RZAFB.[172,173] In RZAFB, electrolyte is continuously circulated through the cell via external tank connected to a pump. The ability to introduce fresh electrolyte into the cell has several advantages, including enhanced efficiency and utilization of the zinc anode by cleaning off the passivating by-products, thereby improving the electrochemical performance of the cell (i.e., high-energy, high-power, coulombic efficiency, long cycle life). Without doubt, RZAFB holds a great future for next-generation RZAB, especially if the pumping system is powered by renewable sources, such as solar or wind energy. This review offers an insight into the strategies needed to design efficient and stable RZABs.

Acknowledgements

Conflict of Interest

The authors declare no conflict of interest.

[1] K. Bradbury, L. Pratson, D. Patino-Echeverri, *Appl. Energy* **2014**, *114*, 512–519.
[2] Y. Li, H. Dai, *Chem. Soc. Rev.* **2014**, *43*, 5257–5275.
[3] D. Stock, S. Dongmo, J. Janek, D. Schrode, *ACS Energy Lett.* **2019**, *4*, 1287–1300.
[4] K. I. Ozoemena, *RSC Adv.* **2016**, 6, 89523–89550
[5] J. Fu, Z. P. Cano, M. G. Park, A. Yu, M. Fowler, Z. Chen, *Adv. Mater.* **2017**, *29*, 1604685.
[6] P. Gu, M. Zheng, Q. Zhao, X. Xiao, H. Hue, H. Pang, *J. Mater. Chem. A* **2017**, *5*, 7651–7666.
[7] A. Sumboja, X. Ge, G. Zheng, F. T. Goh, T. A. Hor, Y. Zong, Z. Liu, *J. Power Sources* **2016**, *332*, 330–336.
[8] D. Yang, D. Chen, Y. Jiang, E. H. Ang, Y. Feng, X. Rui, Y. Yu, *Carbon Energy* **2020**, *3*, 50–65.
[9] M. Luo, W. Sun, B. B. Xu, H. Pan, Y. Jiang, *Adv. Energy Mater.* **2020**, *11*, 2002762.
[10] X. Zhu, C. Hu, R. Amal, L. Dai, X. Lu, *Energy Environ. Sci.* **2020**, *13*, 4536–4563.
[11] J. Song, K. Xu, N. Liu, D. Reed, X. Li, *Mater. Today* **2021**, in press, https://doi.org/10.1016/j.mattod.2020.12.003.
[12] X. Shu, M. Yang, D. Tan, K. S. Hui, K. N. Hiu, J. Zhang, *Mater. Adv.* **2021**, *2*, 96–114.
[13] I. Katsounaros, S. Cherevko, A. R. Zeradjanin, K. J. J. Mayrhofer, *Angew. Chem. Int. Ed.* **2014**, *53*, 102–121; *Angew. Chem.* **2014**, *126*, 104–124.
[14] X. Cai, L. Lai, J. Lin, Z. Shen, *Mater. Horiz.* **2017**, *4*, 945–976.
[15] R. Wang, D. Kirk, G. Zhang, *J. Electrochem. Soc.* **2006**, *153*, C357-C364.
[16] A. L. Zhu, D. P. Wilkinson, X. Zhang, Y. Xing, A. G. Rozhin, S. A. Kulinich, *J. Energy Storage* **2016**, *8*, 35–50.
[17] S. J. Banik, R. Akolkar, *Electrochim. Acta* **2015**, *179*, 475–481.
[18] M. Azhagurajan, A. Nakata, H. Arai, Z. Ogumi, T. Kajita, K. Itoh, K. Itaya, *J. Electrochem. Soc.* **2017**, *164*, A2407-A2417.
[19] H. I. Kim, E. J. Kim, S. J. Kim, H. C. Shin, *J. Appl. Electrochem.* **2015**, *45*, 335–342.
[20] J. Yu, H. Yang, X. Ai, X. Zhu, *J. Power Sources* **2001**, *103*, 93–97.
[21] J. Dobryszycki, S. Biallozor, *Corros. Sci.* **2001**, *43*, 1309–1319.
[22] E. Deiss, F. Holzer, O. Haas, *Electrochim. Acta* **2002**, *47*, 3995–4010.
[23] S. Yang, K. Kim, *J. Electrochem. Sci. Technol.* **2018**, *9*, 334–344.
[24] L. Lei, Y. Sun, X. Wang, Y. Jiang, J. Li, *Front. Mater.* **2020**, *7*, 96.
[25] C. Han, W. Li, H. K. Liu, S. Dou, J. Wang, *Nano Energy* **2020**, *74*, 104880.
[26] L. Hu, P. Xiao, L. Xue, H. Li, T. Zhai, *EnergyChem* **2021**, *3*, 100052.
[27] T. H. Wu, Y. Zhang, Z. D. Althouse, N. Liu, *Mater. Today Nano* **2019**, *6*, 100032.
[28] P. Wang, F. Zhao, H. Chang, Q. Sun, Z. Zhang, *J. Mater. Sci. Mater. Electron.* **2020**, *31*, 17953–17966.
[29] S. Huang, H. Li, P. Pei, K. Wang, Y. Xiao, C. Zhang, C. Chen, *iScience* **2020**, *23*, 101169.
[30] A. R. Mainar, L. C. Colmenares, H. J. Grande, J. A. Blázquez, *Batteries* **2018**, *4*, 46.
[31] D. Deckenbach, J. J. Schneider, *J. Power Sources* **2021**, *488*, 229393.
[32] C. Okuwa, B. Aremo, M. Adeoye, *FUOYE J. Eng. Technol.* **2019**, *4*, DOI:10.46792/fuoyejet.v4i3.519
[33] W. Sun, F. Wang, B. Zhang, M. Zhang, V. Küpers, X. Ji, C. Theile, P. Bieker, K. Xu, C. Wang, M. Winter, *Science* **2021**, *371*, 46–51.
[34] S. Qu, B. Liu, X. Fan, X. Liu, J. Liu, J. Ding, X. Han, Y. Deng, W. Hu, C. Zhong, *ChemistrySelect* **2020**, *5*, 8305–8310.
[35] J. Yu, F. Chen, Q. Tang, T. T. Gebremariam, J. Wang, X. Gong, X. Wang, *ACS Appl. Nano Mater.* **2019**, *2*, 2679–2688.
[36] Y. J. Kim, K. S. Ryu, *Appl. Surf. Sci.* **2019**, *480*, 912–922.
[37] M. Schmid, M. Willert-Porada, *J. Power Sources* **2017**, *351*, 115–122.
[38] Y. J. Min, S. J. Oh, M. S. Kim, J. H. Choi, S. Eom, *Ionics* **2019**, *25*, 1707–1713.
[39] E. O. Aremu, D. J. Park, K. S. Ryu, *Ionics* **2019**, *25*, 4197–4207.
[40] H. E. Lin, C. H. Ho, C. Y. Lee, *Surf. Coat. Technol.* **2017**, *319*, 378–385.
[41] S. Dongmo, D. Stock, J. J. A. Kreissl, M. Groß, S. Weixler, M. Hagen, K. Miyazaki, T. Abe, D. Schroder, *ACS Omega* **2020**, *5*, 626–633.
[42] K. Jayasayee, S. Clark, C. King, P. I. Dahl, J. R. Tolchard, M. Juel, *Processes* **2020**, *8*, 592.
[43] P. Liu, X. Ling, C. Zhong, Y. Deng, X. Han, W. Hu, *Front. Chem.* **2019**, *7*, 656.
[44] J. Zhang, X. L. Li, S. Fan, S. Huang, D. Yan, L. Liu, P. V. Alvarado, H. Y. Yang *Mater. Today* **2020**, *16*, 100407.
[45] T. Schmitt, T. Arlt, I. Manke, A. Latz, B. Horstmann, *J. Power Sources* **2019**, *432*, 119–132.
[46] J. Zhang, Q. Zhou, Y. Tang, L. Zhang, Y. Li, *Chem. Sci.* **2019**, *10*, 8924.
[47] M. Gong, Y. Li, H. Wang, Y. Liang, J. Z. Wu, J. Zhou, J. Wang, T. Regier, F. Wei, H. Dai, *J. Am. Chem. Soc.* **2013**, *135*, 8452–8455.
[48] M. Li, X. Bi, R. Wang, Y. Li, G. Jiang, L. Li, C. Zhong, Z. Chen, J. Lu, *Matter* **2020**, *2*, 32–49.
[49] W. Zhang, Y. Liu, L. Zhang, J. Chen, *Nanomaterials* **2019**, *9*, 1402.
[50] X. Ren, Y. Wang, A. Liu, Z. Zhang, Q. Lv, B. Liu, *J. Mater. Chem. A* **2020**, *8*, 24284–24306.
[51] J. Zhang, Y. Yuan, L. Gao, G. Zeng, M. Li, H. Huang, *Adv. Mater.* **2021**, https://doi.org/10.1002/adma.202006494
[52] P. Pei, K. Wang, Z. Ma, *Appl. Energy* **2014**, *128*, 315–324.
[53] C. Wei, H. Wang, K. Eid, J. Kim, J. H. Kim, Z. A. Alothman, Y. Yamauchi, L. Wang, *Chem. Eur. J.* **2016**, *23*, 637–643.
[54] M. A. Ahsan, T. He, K. Eid, A. M. Abdullah, M. L. Curry, A. Du, A. R. Puente Santiago, L. Echegoyen, J. C. Noveron, *J. Am. Chem. Soc.* **2021**, *143*, 1203–1215.
[55] H. Wang, S. Yin, K. Eid, Y. Li, Y. Xu, X. Li, H. Xue, L. Wang, *ACS Sustainable Chem. Eng.* **2018**, *6*, 11768–11774.
[56] S. Lu, K. Eid, Y. Deng, J. Guo, L. Wang, H. Wang, H. Gu, *J. Mater. Chem. A* **2017**, *5*, 9107–9112.

[57] J. Fu, R. Liang, G. Liu, A. Yu, Z. Bai, L. Yang, Z. Chen, *Adv. Mater.* **2019**, *31*, 1805230.

[58] A. B. Haruna, K. I. Ozoemena, *Curr. Opin. Electrochem.* **2020**, *21*, 219–224.

[59] H. F. Wang, C. Tang, B. Wang, B. Q. Li, Q. Zhang, *Adv. Mater.* **2017**, *29*, 1702327.

[60] Y. Liu, C. Xiao, M. Lyu, Y. Lin, W. Cai, P. Huang, W. Tong, Y. Zou, Y. Xie, *Angew. Chem. Int. Ed.* **2015**, *127*, 11383–11387.

[61] O. Mabayoje, A. Shoola, B. R. Wygant, C. B. Mullins, *ACS Energy Lett.* **2016**, *1*, 195–201.

[62] J. Sun, H. Yin, P. Liu, Y. Wang, X. Yao, Z. Tang, H. Zhao, *Chem. Sci.* **2016**, *7*, 5640.

[63] J. Wu, B. Liu, X. Fan, J. Ding, X. Han, Y. Deng, W. Hu, C. Zhong, *Carbon Energy* **2020**, *2*, 370–386.

[64] J. Ma, Z. Xiang, J. Zhang, *Sci. China Chem.* **2018**, *61*, 592–597.

[65] D. U. Lee, P. Xu, Z. P. Cano, A. G. Kashkooli, M. G. Park, Z. Chen, *J. Mater. Chem. A.* **2016**, *4*, 7107.

[66] G. M. Tomboc, P. Yu, T. Kwon, K. Lee, J. Li, *APL Mater.* **2020**, *8*, 050905.

[67] V. Celorrio, E. Dann, L. Calvillo, D. J. Morgan, S. R. Hall, D. J. Fermin, *ChemElectroChem* **2016**, *3*, 283–291.

[68] J. S. Lee, K. S. Tai, R. Cao, N. S. Choi, M. Liu, K. T. Lee, J. Cho, *Adv. Energy Mater.* **2011**, *1*, 34–50.

[69] N. T. Suen, S. F. Hung, Q. Quan, N. Zhang, Y. J. Xu, H. M. Chen, *Chem. Soc. Rev.* **2017**, *46*, 337–365.

[70] H. B. Yang, J. Miao, S. F. Hung, J. Chen, H. B. Tao, X. Wang, L. Zhang, R. Chen, J. Gao, H. M. Chen, L. Dai, B. Liu, *Sci. Adv.* **2016**, *2*, e1501122.

[71] Z. F. Huang, J. Wang, Y. Peng, C. Y. Jung, A. Fisher, *Adv. Energy Mater.* **2017**, *7*, 1700544.

[72] M. Kim, J. Park, M. Kang, J. Y. Kim, S. W. Lee, *ACS Cent. Sci.* **2020**, *6*, 880–889.

[73] M. Retuerto, F. Calle-Vallejo, L. Pascual, G. Lumbeeck, M. T. Fernandez-Diaz, M. Croft, J. Gopalakrishnan, M. A. Peña, J. Hadermann, M. Greenblatt, S. Rojas, *ACS Appl. Mater. Interfaces* **2019**, *11*, 21454–21464.

[74] Z. Pei, J. Gu, Y. Wang, Z. Tang, Z. Liu, Y. Huang, Y. Huang, J. Zhao, Z. Chen, C. Zhi, *ACS Nano* **2017**, *11*, 6004–6014.

[75] J. Liang, R. F. Zhou, X. M. Chen, Y. H. Tang, S. Z. Qiao, *Adv. Mater.* **2014**, *26*, 6074–6079.

[76] Y. Liang, Y. Li, H. Wang, J. Zhou, J. Wang, T. Regier, H. Dai, *Nat. Mater.* **2011**, *10*, 780.

[77] B. Li, X. Y. Sun, D. Su, *Phys. Chem. Chem. Phys.* **2015**, *17*, 6691–6694.

[78] H. W. Park, D. U. Lee, P. Zamani, M. H. Seo, L. F. Nazar, Z. Chen, *Nano Energy* **2014**, *10*, 192–200.

[79] S. Gupta, W. Kellogg, H. Xu, X. Liu, J. Cho, G. Wu, *Chem. Asian J.* **2016**, *11*, 10–21.

[80] Y. Dai, J. Yu, M. Ni, Z. Shao, *Chem. Phys. Rev.* **2020**, *1*, 011303.

[81] J. Yu, R. Ran, Y. Zhong, W. Zhou, M. Ni, Z. Shao, *Energy Environ. Mater.* **2020**, *3*, 121–145.

[82] Y. Dai, J. Yu, C. Cheng, P. Tan, M. Ni, *Chem. Eng. J.* **2020**, *397*, 125516;

[83] Y. Bu, O. Gwon, G. Nam, H. Jang, S. Kim, Q. Zhong, J. Cho, G. Kim, *ACS Nano* **2017**, *11*, 11594–11601.

[84] Z. Chen, A. Yu, D. Higgins, H. Li, H. Wang, Z. Chen, *Nano Lett.* **2012**, *12*, 1946–1952.

[85] J. Wei, Y. Liang, Y. Hu, B. Kong, J. Zhang, Q. Gu, Y. Tong, X. Wang, S. P. Jiang, H. Wang, *Angew. Chem. Int. Ed.* **2016**, *55*, 1–6; *Angew. Chem.* **2016**, *128*, 1–1.

[86] L. Yang, D. Cheng, H. Xu, X. Zeng, X. Wan, J. Shui, Z. Xiang, D. Cao, *Proc. Nat. Acad. Sci.* **2018**, *115*, 6626–6631.

[87] T. P. Mofokeng, A. K. Ipadeola, Z. N. Tetana, K. I. Ozoemena, *ACS Omega* **2020**, *5*, 20461–20472.

[88] G. Janani, Y. Chae, S. Surendran, Y. Sim, W. Park, J. K. Kim, U. Sim, *Appl. Sci.* **2020**, *10*, 3165.

[89] M. G. Park, D. U. Lee, M. H. Seo, Z. P. Cano, Z. Chen, *Small* **2016**, *12*, 2707–2714'

[90] L. Gaolatlhe, R. Barik, S. C. Ray, K. I. Ozoemena, *J. Electroanal. Chem.* **2020**, *872*, 113863.

[91] Z. Jin, J. Lv, H. Jia, W. Liu, H. Li, Z. Chen, X. Lin, G. Xie, X. Liu, S. Sun, H. J. Qiu, *Small* **2019**, *15*, 1904180.

[92] X. Cui, B. Zhang, C. Zeng, S. Guo, *MRS Commun.* **2018**, *8*, 1230–1235.

[93] D. Wang, Z. Liu, S. Du, Y. Zhang, H. Li, Z. Xiao, W. Chen, R. Chen, Y. Wang, Y. Zou, S. Wang, *J. Mater. Chem. A* **2019**, *7*, 24211–24216.

[94] X. Zhao, Z. Xue, W. Chen, X. Bai, R. Shi, T. Mu, *J. Mater. Chem. A* **2019**, *7*, 26238–26242.

[95] T. Wang, H. Chen, Z. Yang, J. Liang, S. Dai, *J. Am. Chem. Soc.* **2020**, *142*, 4550–4554.

[96] M. W. Glasscott, A. D. Pendergast, S. Goines, A. R. Bishop, A. T. Hoang, C. Renault, J. E. Dick, *Nat. Commun.* **2019**, *10*, 2650.

[97] H. J. Qiu, G. Fang, Y. Wen, P. Liu, G. Xie, X. Liu, S. Sun, *J. Mater. Chem. A* **2019**, *7*, 6499–6506.

[98] S. Li, X. Tang, H. Jia, H. Li, G. Xie, X. Liu, X. Lin, H. J. Qiu, *J. Catal.* **2020**, *383*, 164–171.

[99] T. Loffler, A. Savan, H. Meyer, M. Meischein, V. Strotkotter, A. Ludwig, W. Schuhmann, *Angew. Chem. Int. Ed.* **2020**, *59*, 5844–5850; *Angew. Chem.* **2020**, *132*, 5893–5900.

[100] G. Fang, J. Gao, J. Lv, H. Jia, H. Li, W. Liu, G. Xie, Z. Chen, Y. Huang, Q. Yuan, X. Liu, X. Lin, S. Sun, H. J. Qiu, *Appl. Catal. B* **2020**, *268*, 118431.

[101] Z. Jin, J. Lyu, Y. L. Zhao, H. Li, Z. Chen, X. Lin, G. Xie, X. Liu, J. J. Kai, H. J. Qiu, *Chem. Mater.* **2021**, *33*, 1771–1780.

[102] A. R. Mainar, L. C. Colmenares, O. Leonet, F. Alcaide, J. J. Iruin, S. Weinberger, V. Hacker, E. Iruin, I. Urdanpilleta, J. A. Blazquez, *Electrochim. Acta* **2016**, *217*, 80–91.

[103] J. Liu, L. Jiang, T. Zhang, J. Jin, L. Yuan, G. Sun, *Electrochim. Acta* **2016**, *205*, 38–44.

[104] K. Selvakumar, S. M. S. Kumar, R. Thangamuthu, G. Kruthika, P. Murugan, *Int. J. Hydrogen Energy* **2014**, *39*, 21024–21036.

[105] H. Pan, Y. Shao, P. Yan, Y. Cheng, K. S. Han, Z. Nie, C. Wang, J. Yang, X. Li, P. Bhattacharya, K. T. Mueller, J. Liu, *Nat. Energy* **2016**, *1*, 16039.

[106] X. Chen, L. Wang, H. Li, F. Cheng, J. Chen, *J. Energy Chem.* **2019**, *38*, 20–25.

[107] Y. Zhong, Z. Pan, X. Wang, J. Yang, Y. Qiu, S. Xu, Y. Lu, Q. Huang, W. Li, *Adv. Sci.* **2019**, *6*, 1802243.

[108] P. K. Gangadharan, S. N. Bhange, N. Kabeer, R. Illathvalappil, S. Kurungot, *Nanoscale Adv.* **2019**, *1*, 3243–251.

[109] M. H. Seo, M. G. Park, D. U. Lee, X. Wang, W. Ahn, S. H. Noh, S. M. Choi, Z. P. Cano, B. Han, Z. Chen, *Appl. Catal. B* **2018**, *239*, 677–687.

[110] S. Song, W. Li, Y. P. Deng, Y. Ruan, Y. Zhang, X. Qin, Z. Chen, *Nano Energy* **2020**, *67*, 104208.

[111] X. F. Lu, S. L. Zhang, E. Shangguan, P. Zhang, S. Gao, X. W. Lou, *Adv. Sci.* **2020**, *7*, 2001178.

[112] J. Zhang, X. Bai, T. Wang, W. Xiao, P. Xi, J. Wang, D. Gao, J. Wang, *Nano-Micro Lett.* **2019**, *11*, 2.

[113] X. He, Y. Tian, Z. Huang, L. Xu, J. Wu, J. Qian, J. Zhang, H. Li, *J. Mater. Chem. A* **2021**, *9*, 2301–2307.

[114] L. Diao, T. Yang, B. Chen, B. Zhang, N. Zhao, C. Shi, E. Liu, L. Ma, C. He, *J. Mater. Chem. A* **2019**, *7*, 21232–21243.

[115] G. Fu, Y. Wang, Y. Tang, K. Zhou, J. B. Goodenough, J. M. Lee, *ACS Materials Lett.* **2019**, *1*, 123–131.

[116] Y. He, X. Liu, A. Yan, H. Wan, G. Chen, J. Pan, N. Zhang, T. Qiu, R. Ma, G. Qiu, *ACS Sustainable Chem. Eng.* **2019**, *7*, 19612–19620.

[117] X. Zhu, D. Zhang, C. J. Chen, Q. Zhang, R. S. Liu, Z. Xia, L. Dai, R. Amal, X. Lu, *Nano Energy* **2020**, *71*, 104597.

[118] A. Wang, C. Zhao, M. Yu, W. Wang, *Appl. Catal. B* **2021**, *281*, 119514.

[119] X. Tang, R. Cao, I. Li, B. Huang, W. Zhai, K. Yuan, Y. Chen, *J. Mater. Chem. A* **2020**, *8*, 25919–25930

[120] P. Tan, B. Chen, H. Xu, H. Zhang, W. Cai, M. Ni, M. Liu, Z. Shao, *Energy Environ. Sci.* **2017**, *10*, 2056–2080.

[121] A. T. Al-Hinai, M. H. Al-Hinai, J. Dutta, *Mater. Res. Bull.* **2014**, *49*, 645–650.

[122] A. R. Mainar, O. Leonet, M. Bengoechea, I. Boyano, I. De Meatza, A. Kvasha, A. Guerfi, J. A. Blázquez, *Int. J. Energy Res.* **2016**, *40*, 1032–1049.

[123] N. Shaigan, W. Qu, T. Takeda, *ECS Trans.* **2010**, *28*, 35.

[124] A. K. Ipadeola, K. I. Ozoemena, *RSC Adv.* **2020**, *10*, 17359–17368.

[125] A. K. Ipadeola, P. Mwonga, S. C. Ray, R. R. Maphanga, K. I. Ozoemena, *Electroanalysis* **2020**, *32*, 3060–3074.

[126] M. Mokaddem, P. Volovitch, K. Ogle, *Electrochim. Acta* **2010**, *55*, 7867–7875.

[127] J. J. Xu, H. Ye, J. Huang, *Electrochem. Commun.* **2005**, *7*, 1309–1317.

[128] D. Boden, C. Venuto, D. Wisler, R. Wylie, *J. Electrochem. Soc.* **1968**, *115*, 333.

[129] A. Sumboja, X. Ge, G. Zheng, F. T. Goh, T. A. Hor, Y. Zong, Z. Liu, *J. Power Sources* **2016**, *332*, 330–336.

[130] A. Velichenko, J. Portillo, M. Sarret, C. Muller, *J. Appl. Electrochem.* **1999**, *29*, 1119–1123.

[131] M. Kar, B. Winther-Jensen, M. Forsyth, D. R. MacFarlane, *Phys. Chem. Chem. Phys.* **2013**, *15*, 7191–7197.

[132] K. Deng, Q. Zeng, D. Wang, Z. Liu, G. Wang, Z. Qiu, Y. Zhang, M. Xiao, Y. Meng, *J. Mater. Chem. A* **2020**, *8*, 1557–1577.

[133] A. Guerfi, J. Trottier, I. Boyano, I. De Meatza, J. Blazquez, S. Brewer, K. Ryder, A. Vijh, K. Zaghib, *J. Power Sources* **2014**, *248*, 1099–1104.

ChemElectroChem

Review
doi.org/10.1002/celc.202100574

Chemistry Europe
European Chemical
Societies Publishing

[134] M. S. Chae, J. W. Heo, H. H. Kwak, H. Lee, S. Hong, *J. Power Sources* **2017**, *337*, 204–211.

[135] N. Vassal, E. Salmon, J. Fauvarque, *Electrochim. Acta* **2000**, *45*, 1527–1532.

[136] J. Fu, Z. P. Cano, M. G. Park, A. Yu, M. Fowler, Z. Chen, *Adv. Mater.* **2017**, *29*, 1604685.

[137] G. Stone, S. Mullin, A. Teran, D. Hallinan Jr, A. Minor, A. Hexemer, N. Balsara, *J. Electrochem. Soc.* **2011**, *159*, A222.

[138] J. Fauvarque, S. Guinot, N. Bouzir, E. Salmon, J. Penneau, *Electrochim. Acta* **1995**, *40*, 2449–2453.

[139] S. S. Zhang, D. Foster, J. Read, *J. Power Sources* **2010**, *195*, 1235–1240.

[140] N. S. Schauser, R. Seshadri, R. A. Segalman, *Mol. Syst. Des. Eng.* **2019**, *4*, 263–279.

[141] S. Ikeda, Y. Mori, Y. Furuhashi, H. Masuda, O. Yamamoto, *J. Power Sources* **1999**, *81*, 720–723.

[142] J. Dupont, R. F. de Souza, P. A. Suarez, *Chem. Rev.* **2002**, *102*, 3667–3692.

[143] M. M. Hossain, E. H. B. Anari, L. Aldous, *Electrochem. Commun.* **2013**, *34*, 331–334.

[144] M. C. Buzzeo, R. G. Evans, R. G. Compton, *ChemPhysChem* **2004**, *5*, 1106–1120.

[145] Z. Liu, T. Cui, T. Lu, M. Shapouri Ghazvini, F. Endres, *J. Phys. Chem. C* **2016**, *120*, 20224–20231.

[146] E. L. Smith, A. P. Abbott, K. S. Ryder, *Chem. Rev.* **2014**, *114*, 11060–11082.

[147] W. Kao-ian, R. Pornprasertsuk, P. Thamyongkit, T. Maiyalagan, S. Kheawhom, *J. Electrochem. Soc.* **2019**, *166*, A1063.

[148] H. Qiu, X. Du, J. Zhao, Y. Wang, J. Ju, Z. Chen, Z. Hu, D. Yan, X. Zhou, G. Cui, *Nat. Commun.* **2019**, *10*, 1–12.

[149] C. Cachet, B. Saidani, R. Wiart, *J. Electrochem. Soc.* **1992**, *139*, 644.

[150] F. R. McLarnon, E. J. Cairns, *J. Electrochem. Soc.* **1991**, *138*, 645.

[151] H. Yang, Y. Cao, X. Ai, L. Xiao, *J. Power Sources* **2004**, *128*, 97–101.

[152] R. K. Ghavami, Z. Rafiei, S. M. Tabatabaei, *J. Power Sources* **2007**, *164*, 934–946.

[153] J. Lee, S. Tai Kim, R. Cao, N. Choi, M. Liu, K. T. Lee, J. Cho, *Adv. Energy Mater.* **2011**, *1*, 34–50.

[154] J. Drillet, F. Holzer, T. Kallis, S. Müller, V. Schmidt, *Phys. Chem. Chem. Phys.* **2001**, *3*, 368–371.

[155] H. H. Cheng, C. Tan, *J. Power Sources* **2006**, *162*, 1431–1436.

[156] L. Kucka, E. Y. Kenig, A. Gorak, *Ind. Eng. Chem. Res.* **2002**, *41*, 5952–5957.

[157] D. Schröder, N. N. S. Borker, M. König, U. Krewer, *J. Appl. Electrochem.* **2015**, *45*, 427–437.

[158] M. A. Rahman, X. Wang, C. Wen, *J. Electrochem. Soc.* **2013**, *160*, A1759.

[159] K. Wippermann, J. Schultze, R. Kessel, J. Penninger, *Corros. Sci.* **1991**, *32*, 205–230.

[160] S. Thomas, N. Birbilis, M. Venkatraman, I. Cole, *J. Sci. Eng.* **2012**, *68*, 015009.

[161] F. R. McLarnon, E. J. Cairns, *J. Electrochem. Soc.* **1991**, *138*, 645.

[162] C. W. Lee, K. Sathiyanarayanan, S. W. Eom, H. S. Kim, M. S. Yun, *J. Power Sources* **2006**, *159*, 1474–477.

[163] M. A. Deyab, G. Mele, *J. Power Sources* **2019**, *443*, 227264.

[164] S. A. Mamuru, K. I. Ozoemena, *Electrochem. Commun.* **2010**, 12, 1539–1542.

[165] O. O. Fashedemi, K. I. Ozoemena, *Phys. Chem. Chem. Phys.* **2013**, 15, 20982–20991

[166] O. O. Fashedemi, K. I. Ozoemena, *RSC Adv.* **2015**, 5, 22869–22878.

[167] J. Masa, K. Ozoemena, W. Schuhmann, J. H. Zagal, *J. Porphyrins Phthalocyanines* **2012**, 16: 761–784.

[168] G. Chen, Y. Xu, L. Huang, A. I. Douka, B. Y. Xia, *J. Energy Chem.* **2021**, *55*, 183–189

[169] W. Ling, P. Wang, Z. Chen, H. Wang, J. Wang, Z. Ji, J. Fei, Z. Ma, N. He, Y. Huang, *ChemElectroChem* **2020**, 7, 2957–2978.

[170] J. Lv, S. C. Abbas, Y. Huang, Q. Liu, M. Wu, Y. Wang, L. Dai, *Nano Energy* **2018**, *43*, 130.

[171] X. Liu, Y. Yuan, J. Liu, B. Liu, X. Chen, J. Ding, X. Han, Y. Deng, C. Zhong, W. Hu, *Nat. Commun.* **2019**, *10*, 4767.

[172] Y. Cheng, D. Li, L. Shi, Z. Xiang, *Nano Energy* **2018**, *47*, 361–367.

[173] X. Han, X. Li, J. White, C. Zhong, Y. Deng, W. Hu, T. Ma, *Adv. Energy Mater.* **2018**, *8*, 1801396.